nature methods

ARTICLES

https://doi.org/10.1038/s41592-020-01005-2

Click-ExM enables expansion microscopy for all biomolecules

De-en Sun[1,2], Xinqi Fan[1,2], Yujie Shi[1,2,7], Hao Zhang[1,2], Zhimin Huang[1,3], Bo Cheng[1,2], Qi Tang[1,2], Wei Li[1,2], Yuntao Zhu[1,2,8], Jinyi Bai[1,3], Wei Liu[4], Yuan Li[4], Xiaoting Wang[4], Xiaoguang Lei[1,2,3,5,6] and Xing Chen[1,2,3,5,6] ✉

Expansion microscopy (ExM) allows super-resolution imaging on conventional fluorescence microscopes, but has been limited to proteins and nucleic acids. Here we develop click-ExM, which integrates click labeling into ExM to enable a 'one-stop-shop' method for nanoscale imaging of various types of biomolecule. By click labeling with biotin and staining with fluorescently labeled streptavidin, a large range of biomolecules can be imaged by the standard ExM procedure normally used for proteins. Using 18 clickable labels, we demonstrate click-ExM on lipids, glycans, proteins, DNA, RNA and small molecules. We demonstrate that click-ExM is applicable in cell culture systems and for tissue imaging. We further show that click-ExM is compatible with signal-amplification techniques and two-color imaging. Click-ExM thus provides a convenient and versatile method for super-resolution imaging, which may be routinely used for cell and tissue samples.

By physically expanding proteins or RNA of fixed specimens embedded in a swellable polymer hydrogel, expansion microscopy (ExM) enables nanoscale imaging on conventional diffraction-limited microscopes[1–6]. As a critical step of ExM, the biomolecules or the labeled fluorophores need to be covalently anchored into the polymer network during gelation. Furthermore, they have to survive the step of homogenization of the fixed cells (for example, by strong protease digestion), an essential step to ensure isotropic expansion. Although tailored protocols have been developed for ExM imaging of proteins and RNA, other types of biomolecule such as lipids, glycans and small molecules remain challenging to image by ExM.

To expand the applicability of ExM, we herein develop click-ExM, a variant of ExM that combines click labeling and ExM to enable super-resolution imaging of various kinds of biomolecules in a unified procedure (Fig. 1). We demonstrate click-ExM for imaging lipids, glycans, proteins, nucleic acids and small molecules. Furthermore, click-ExM imaging of lipids and proteins is performed on the mouse brain tissue. In addition, signal-amplification techniques can be implemented in click-ExM to overcome the issue of volumetric dilution of fluorescence intensity induced by expansion. Finally, two-color click-ExM imaging is demonstrated.

Results

Development of click-ExM. To develop a unified protocol for labeling, anchoring and preserving fluorescent signals for different biomolecules, we exploited click labeling, which has emerged as a versatile tool for fluorescence imaging of various kinds of biomolecule[7]. DNA, RNA, proteins, glycans and lipids can all be metabolically labeled with a bioorthogonal or 'clickable' functional group (for example, azide or alkyne), which is subsequently conjugated with fluorescent probes via bioorthogonal chemistry such as Cu(I)-catalyzed azide-alkyne cycloaddition (CuAAC or click chemistry)[8,9] and copper-free click chemistry[10] (Supplementary Fig. 1). In addition, bioorthogonal functional groups can also be site-specifically incorporated into proteins by using strategies such as genetic code expansion[11]. In click-ExM, the metabolically or genetically labeled biomolecules are reacted with azide-biotin or alkyne-biotin via click chemistry, followed by staining with fluorescently labeled streptavidin (Fig. 1 and Supplementary Fig. 2). The streptavidin–fluorophore conjugates serve as a trifunctional probe, which binds biotin, anchors into the gel and presents fluorescence. Glutaraldehyde (GA) or the succinimidyl ester of 6-((acryloyl)amino)hexanoic acid (AcX) reacts with the lysine residues of streptavidin and provides the anchoring groups. Up to 14 acryloyl groups were conjugated onto streptavidin by using AcX as the anchoring agent, ensuring efficient incorporation during gelation (Supplementary Fig. 3a,b). The core structure of streptavidin was resistant to strong protease digestion (that is, by proteinase K) (Supplementary Fig. 3c), consistent with the previously observed preservation of streptavidin in protein-retention ExM (proExM)[4]. These results indicate that streptavidin can be readily cross-linked into the gel and survive through homogenization and expansion.

The proExM protocol was adapted for click-ExM[4,5] (Extended Data Fig. 1). The expansion factor was determined by two methods. The same cells were imaged both pre- and postexpansion, from which the expansion factor, termed sEF, was calculated either from the transformation matrix (for samples with rigid registration) or distances of paired landmarks (for samples without registration) (Extended Data Fig. 1a,g). Alternatively, the expansion factor was quantified by measuring the gel size before and after expansion, which was termed gEF (Extended Data Fig. 1j). In this work,

[1]College of Chemistry and Molecular Engineering, Peking University, Beijing, China. [2]Beijing National Laboratory for Molecular Sciences, Peking University, Beijing, China. [3]Peking-Tsinghua Center for Life Sciences, Peking University, Beijing, China. [4]School of Life Sciences, Peking University, Beijing, China. [5]Synthetic and Functional Biomolecules Center, Peking University, Beijing, China. [6]Key Laboratory of Bioorganic Chemistry and Molecular Engineering of Ministry of Education, Peking University, Beijing, China. [7]Present address: Department of Molecular Medicine, The Scripps Research Institute, La Jolla, CA, USA. [8]Present address: Department of Biomolecular Systems, Max Planck Institute of Colloids and Interfaces, Potsdam, Germany. ✉e-mail: xingchen@pku.edu.cn

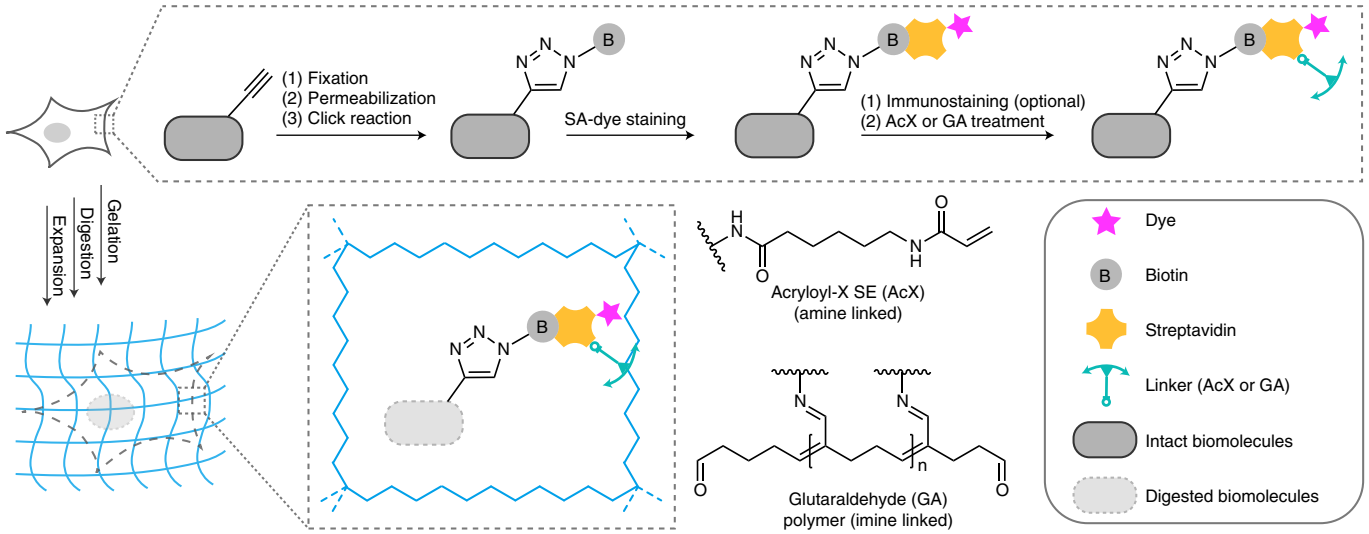

Fig. 1 | Schematic of the click-ExM workflow. After metabolic or genetic labeling of biomolecules with alkynes (or azides, Supplementary Fig. 2), the cells are reacted with azide-biotin via click chemistry and stained with streptavidin-dye conjugates (SA-dye staining), followed by the standard ExM procedure.

gEF was kept constant (4.5 ± 0.1) for all click-ExM and proExM experiments.

Click-ExM imaging of lipids. We first demonstrated click-ExM for imaging lipids, a major biomacromolecule that has not been visualized by ExM. COS-7 cells were treated with alkyne-choline (Alk-Cho) to metabolically label Cho-containing phospholipids, the most abundant phospholipids in cellular membranes[12] (Fig. 2a). After reacting the incorporated Alk-Cho with azide-TAMRA, the membranes could be visualized by confocal microscopy before expansion, but the fluorescence was completely lost after the standard ExM procedure (Extended Data Fig. 2a,b). Membrane staining confirmed that lipids could not be retained through the expansion process in ExM (Extended Data Fig. 2c). We therefore applied click-ExM, in which the Alk-Cho-treated cells were fixed and permeabilized with saponin, followed by click reaction with azide-biotin, staining with streptavidin-Alexa Fluor 555 (AF555), and AcX or GA treatment (Fig. 1). After gelation, digestion and expansion, the AF555 fluorescence was well preserved and the Alk-Cho-incorporated membranes were visualized with super resolution (Fig. 2 and Extended Data Figs. 2d and 3a–i). The click-ExM procedure preserved the fluorescence signal with high efficiency, approximately 60%, which was comparable to proExM (Supplementary Note 1). Furthermore, the lipid structures resolved by click-ExM agreed well with those observed by conventional super-resolution techniques (Supplementary Note 1).

By costaining of the mitochondrial markers, the distribution of Cho-containing phospholipids on the outer membrane of mitochondria was clearly observed by multicolor proExM and click-ExM (Fig. 2b,c and Extended Data Fig. 3a). Similarly, the structures of endoplasmic reticulum and Golgi apparatus could be resolved by click-ExM (Fig. 2d–g and Extended Data Fig. 3b,c). For click-ExM of Cho-containing phospholipids, sEF determined by imaging the same cells pre- and postexpansion was 4.4, in good agreement with gEF (Extended Data Fig. 3d,e). The root mean square (r.m.s.) error of feature measurements over length scales from 0 to 7.5 µm after click-ExM were within 2% of the measurement distance, which demonstrated high isotropy of click-ExM (Extended Data Fig. 3f).

We then applied click-ExM to rat cardiomyocytes treated with Alk-Cho, in which the network of interconnected and highly dense mitochondria were visualized (Fig. 2h–j and Extended Data Fig. 3g–i). Furthermore, click-ExM was applied to the brain tissue. Acute mouse brain slices were metabolically labeled with Alk-Cho, and click-ExM revealed membraneous structures of cellular networks, which were continuously traced (Extended Data Fig. 4).

Various lipid reporters including Alk-palmitic acid, Alk-farnesol, Alk-myristic acid and Alk-stearic acid have been developed for labeling fatty acids and prenol lipids[13–16]. Click-ExM using these lipid reporters enabled super-resolution imaging of the distribution of the corresponding fatty acids or prenol lipids in COS-7 and HeLa cells (Extended Data Fig. 3j). In addition, protein carbonylation by 4-hydroxy-2-nonenal (HNE), a lipid-derived electrophile that reacts with cysteine residues, was visualized by click-ExM by conjugating the resulting aldehyde group on proteins with aminooxy-alkyne[17] (AOyne, Extended Data Fig. 3k). These results demonstrate the broad use of click-ExM in lipid imaging.

Signal amplification for click-ExM. The volumetric dilution of fluorophores in ExM reduces the signal intensity, a disadvantage that can be overcome by signal-amplification techniques. Because amplification by immunosignal hybridization chain reaction (isHCR) has been demonstrated on streptavidin with the biotin–DNA HCR initiator conjugate[18], click-ExM is compatible with isHCR (Extended Data Fig. 5a). Furthermore, we developed a controllable signal-amplification protocol by exploiting the multivalence of streptavidin (Extended Data Fig. 5b). By synthesizing a biotin trimer (Supplementary Note 2), streptavidin staining could be iteratively performed with the signal gradually increased in each round of amplification (Extended Data Fig. 5c).

Click-ExM imaging of glycans. Next, we applied click-ExM for imaging glycans, another major biomacromolecule not yet amenable to ExM. The sialoglycans on the membrane of HeLa cells were metabolically labeled with azido sialic acid (SiaNAz, Extended Data Fig. 6a) or *N*-azidoacetylmannosamine (ManNAz) (Fig. 3a), the metabolic precursor of SiaNAz[19,20]. Of note, unprotected azido sugars were used in this work to avoid nonspecific S-glyco-modification induced by per-*O*-acetylation[21,22]. Click-ExM revealed that the SiaNAz-labeled glycans were widely distributed on the basal plasma membrane (Extended Data Fig. 6b). The sialoglycans on the hollow membrane protrusions such as microvilli were clearly resolved by the nanoscale resolution of click-ExM (Fig. 3b). These observations were consistent with earlier studies on sialoglycans using localization-based super-resolution microscopy[23–25].

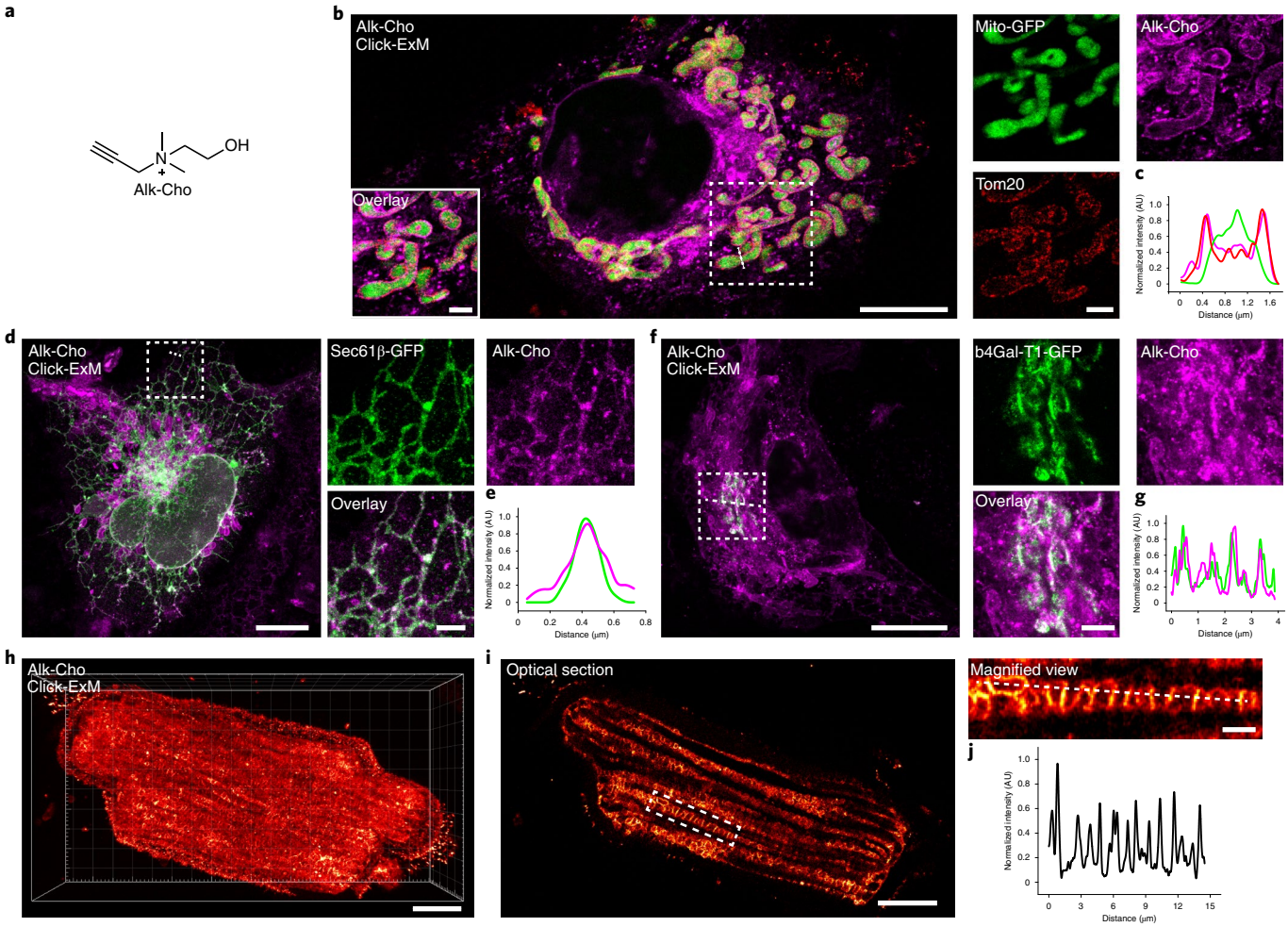

Fig. 2 | Click-ExM imaging of lipids. a, Chemical structure of Alk-Cho. **b**, Click-ExM images of Alk-Cho-labeled phospholipids (AF555, magenta) in COS-7 cells. Mito-GFP (green) was expressed in the mitochondrial matrix and Tom20 located in the mitochondrial outer membrane was immunostained with AF647 (red, staining after gelation and digestion, see Methods). **c**, Fluorescence intensity profiles of mito-GFP (green), Alk-Cho (magenta) and Tom20 (red) along the dotted line in **b**. AU, arbitrary units. **d**, Click-ExM images of Alk-Cho-labeled phospholipids (AF555, magenta) and endoplasmic reticulum-expressing Sec61β-GFP (green) in COS-7 cells. **e**, Fluorescence intensity profiles of Sec61β-GFP (green) and Alk-Cho (magenta) along the dotted line in **d**. **f**, Click-ExM images of Alk-Cho-labeled phospholipids (AF555, magenta) and Golgi expressing b4Gal-T1-GFP (green) in COS-7 cells. **g**, Fluorescence intensity profiles of b4Gal-T1-GFP (green) and Alk-Cho (magenta) along the dotted line in **f**. **h**, 3D click-ExM image of Alk-Cho-labeled phospholipids (AF555, red hot) in rat cardiomyocytes. **i**, Optical section of **h** and zoomed-in view of the boxed region. **j**, Fluorescence profile of Alk-Cho (magenta) along the dotted line in **i**. Scale bars, 10 μm (**b**,**d**,**f**,**h**,**i**) and 2 μm (insets of **b**,**d**,**f**,**i**). All distances and scale bars are corresponding to pre-expansion dimension based on gEF. GA was used for anchoring. Representative images from three or more (**h**,**i**) or two (**b**,**d**,**f**) independent experiments.

Click-ExM imaging of sialoglycans was then performed on rat hippocampal neurons treated with ManNAz. With click-ExM, the tube-like structure of neurites with a diameter of roughly 500 nm was readily and clearly delineated by sialoglycans on the membrane (Fig. 3c, top). By contrast, the tubular structure was unresolvable before expansion (Fig. 3c, bottom). In rat cardiomyocytes that had a relatively low labeling with ManNAz, click-ExM with isHCR amplification revealed sialoglycans on the orderly spaced transverse tubule (T-tubule) network (Fig. 3d, top), with a much better resolution than conventional confocal microscopy[26] (Fig. 3d, bottom and Extended Data Fig. 6c).

We then applied click-ExM for imaging O-GlcNAcylation, modification of serine and threonine residues with an *N*-acetylglucosamine (GlcNAc) monosaccharide, which occurs on various intracellular proteins[27]. HeLa cells were treated with *N*-azidoacetylgalactosamine (GalNAz) (Fig. 3a), which metabolically labeled both cell-surface glycans and O-GlcNAc[28,29]. After click reaction with alkyne-biotin and staining with streptavidin-dye conjugates, fluorescence was observed in the cytoplasm and nucleus, presumably from the labeled O-GlcNAc (Fig. 3e and Extended Data Fig. 6d). Nucleoporins, the constituent building blocks of the nuclear pore complex (NPC), are heavily O-GlcNAcylated and can be stained by the O-GlcNAc-recognizing lectin wheat germ agglutinin, which has been used for super-resolution imaging of the central channel of NPC[30]. Heavy GalNAz labeling was colocalized with NPC staining on the nuclear envelop (Extended Data Fig. 6e). Using click-ExM, individual NPC was resolved with a diameter of around 113.5 nm by metabolic O-GlcNAc labeling (Fig. 3f–h). Moreover, click-ExM of ManNAz- and GalNAz-labeled cells exhibited high isotropy (Extended Data Fig. 6f–k).

Click-ExM imaging of O-GlcNAc could also be performed by using the chemoenzymatic method based on a mutant galactosyltransferase (Y289L GalT1) to label O-GlcNAc with GalNAz[31] (Extended Data Fig. 6l). In addition, click-ExM in combination with chemoenzymatic labeling was generally applicable for nanoscale imaging of other glycans, such as the cancer-associated

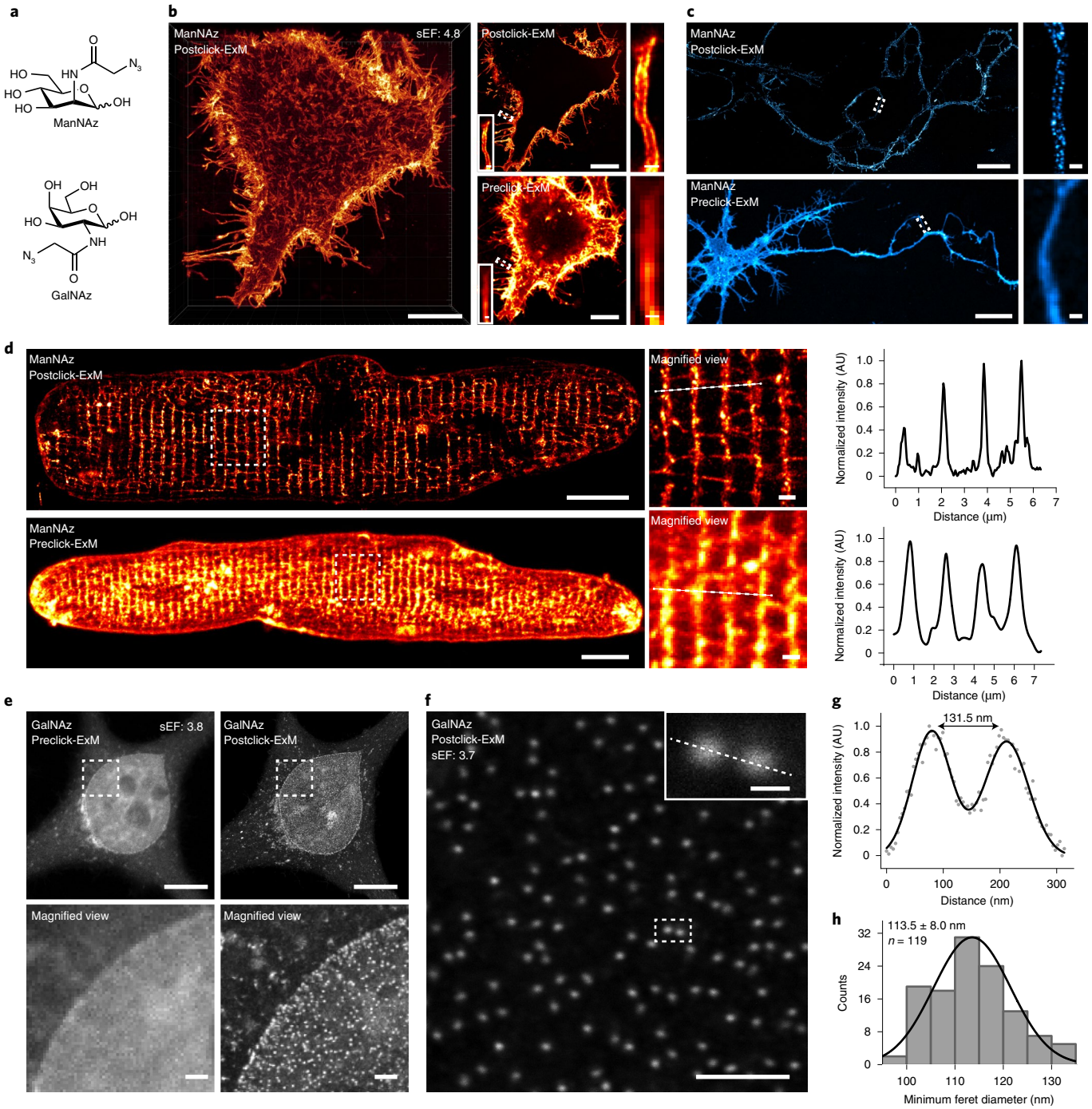

Fig. 3 | Click-ExM imaging of glycans. a, Chemical structures of ManNAz and GalNAz. **b**, Pre- and postclick-ExM images of sialoglycans (AF488, red hot) in ManNAz-treated HeLa cells. 3D image (left), optical section (middle) and zoomed-in images of a microvillus (right) are shown. **c**, Pre- and postclick-ExM images of sialoglycans (AF488, cyan hot) in ManNAz-treated rat hippocampus neurons. zoomed-in images of a neurite in the boxed regions are shown on the right. **d**, Pre- and postclick-ExM images of sialoglycans (AF546, red hot) in ManNAz-treated rat cardiomyocytes after isHCR amplification. Fluorescence profiles along the dotted lines in the boxed regions are shown. **e**, Pre- and postclick-ExM images of O-GlcNAc (AF488, gray) in GalNAz-treated HeLa cells. **f**, Click-ExM images of GalNAz-labeled nucleoporins (AF488, gray) in HeLa cells. **g**, Fluorescence profile of along the dotted line in **f**. **h**, Distribution of minimum Feret diameter of GalNAz-labeled nucleoporins in **f**. AcX (**b**,**e**,**f**) or GA (**c**,**d**) was used for anchoring. Scale bars, 20 μm (**c**), 10 μm (**b**,**d**,**e**), 1 μm (inset of **c**–**e**,**f**), 500 nm (inset of **b**) and 100 nm (inset of **f**). All distances and scale bars correspond to the pre-expansion dimension based on sEF (**b**,**e**–**h**) or gEF (**c**,**d**). Representative images from ≥3 (**b**,**d**–**f**, preclick-ExM of **c**) or 2 (postclick-ExM of **c**) independent experiments.

N-acetyllactosamine (LacNAc) on the surface of HeLa cells[32] (Extended Data Fig. 6m). Of note, the LacNAc level was relatively low and the signal was amplified by the iterative biotin-streptavidin staining method.

Click-ExM imaging of proteins. To demonstrate the applicability of click-ExM for protein imaging, U2OS and HeLa cells, rat cortical neurons and acute mouse brain slices were treated with azidohomoalanine (AHA) (Fig. 4a), a noncanonical amino acid serving

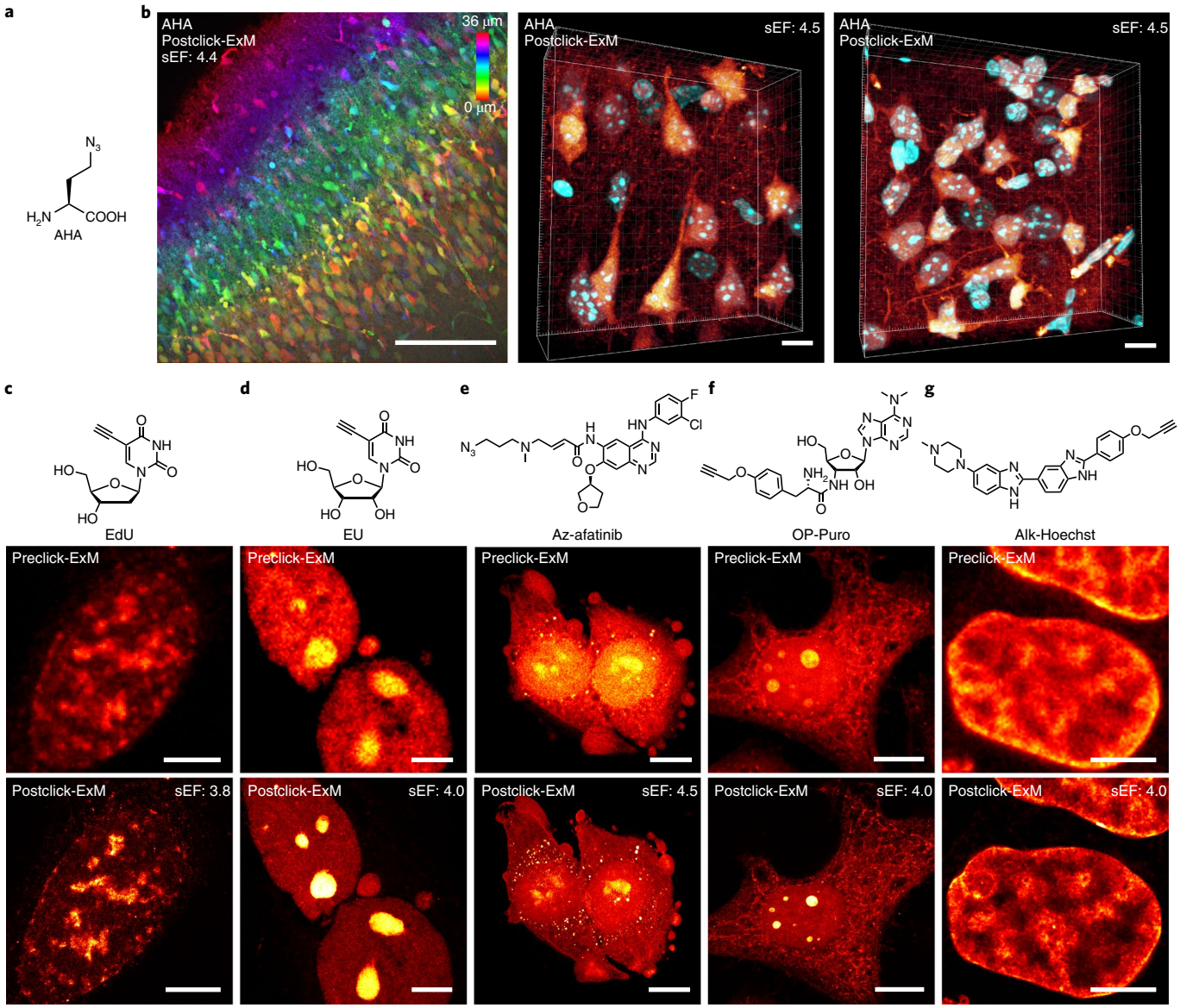

Fig. 4 | Click-ExM imaging of proteins, nucleic acids and small molecules. a, Chemical structure of AHA. **b**, Acute mouse brain slices with a thickness of 150 µm were metabolically labeled with AHA. Postclick-ExM image with an imaging depth of around 36 µm (left) and 3D rendering images of postclick-ExM (middle and right) are shown. Nascent proteins were stained with SA-AF488 (left) or with SA-AF555 (middle and right). Images were acquired using a ×10/0.75-NA air objective (left) or a ×40/1.10-NA water objective (middle and right). The nuclei were stained with Hoechst 33342 (cyan, middle and right). Representative images from three or more slices. **c**, Chemical structure of EdU, and pre- and postclick-ExM images of nascent DNA (AF488, red hot) in EdU-treated HeLa cells. **d**, Chemical structure of EU, and pre- and postclick-ExM images of nascent RNA (AF555, red hot) in EU-treated HeLa cells. **e**, Chemical structure of Az-afatinib, and pre- and postclick-ExM images of HeLa cells treated with Az-afatinib (AF555, red hot). **f**, Chemical structure of OP-Puro, and pre- and postclick-ExM images of nascent peptides (AF488, red hot) in OP-Puro-treated HeLa cells. **g**, Chemical structure of Alk-Hoechst, and pre- and postclick-ExM images of DNA (AF488, red hot) in Alk-Hoechst-labeled HeLa cells. AcX was used for anchoring. Scale bars, 100 µm (**b** left), 10 µm (**b** middle and right, **e**,**f**) and 5 µm (**c**,**d**,**g**). All distances and scale bars correspond to the pre-expansion dimension based on sEF. Representative images from three or more independent experiments.

as a surrogate for methionine, to metabolically label nascent proteins[33]. Click-ExM imaging revealed the distribution of newly synthesized proteins in both cell and tissue samples with high resolution (Fig. 4b and Extended Data Fig. 7a–e). While the streptavidin-based click-ExM serves a unified protocol for various biomolecules, click-ExM could also be performed by direct click labeling with fluorophores for those that can be anchored into the gel, such as proteins (Extended Data Fig. 7b). Furthermore, click-ExM is applicable for imaging specific proteins. Using the genetic code expansion strategy based on the pyrrolysine system, three proteins including geen fluorescent protein (GFP), histone H2B and GTPase KRas were site-specifically incorporated with an alkyne-containing pyrrolysine analog[34] (Extended Data Fig. 7f). Click-ExM resolved the cellular distributions of these proteins (Extended Data Fig. 7g).

Click-ExM imaging of nucleic acids. For nucleic acid imaging, we used 5-ethynyl-2′-deoxyuridine (EdU) to metabolically label nascent DNA[35]. Under click-ExM, the fine structure of chromatin in cell nuclei was resolved with low distortion (Fig. 4c and Extended Data Fig. 8a–c). With super resolution, the distribution

of heterochromatin and euchromatin was differentiated. During S phase, EdU labeling and click-ExM clearly revealed the boundaries of replication domains, which are coreplicating Mb-sized segments of chromosomal DNA (Extended Data Fig. 8d). By using multicolor click-ExM, we showed that the newly synthesized DNA was largely colocalized with histone H3 (Extended Data Fig. 8e). In addition, nascent RNA in HeLa cells was metabolically incorporated with 5-ethynyluridine (EU)[36] and visualized by click-ExM with little distortion (Fig. 4d and Extended Data Fig. 8f–h). In the nucleus, intense labeling in nucleoli, presumably from preribosomal RNA, and diffused labeling in the nucleoplasm, presumably from messenger RNA, were observed at nanoscale resolution.

Click-ExM imaging of small molecules. In addition to biomacromolecules, we envisioned that click-ExM would enable super-resolution imaging of small molecules, including drugs, metabolites and chemical probes, in the cells. The small molecules should tolerate modification with an azide or alkyne without interfering with their function and cellular localization. Afatinib is an irreversible inhibitor for ErbB family and has been approved by the Food and Drug Administration to treat metastatic non-small cell lung cancer with nonresistant epidermal growth factor receptor mutations[37]. We installed an azide at the *N*-methyl position so that the activity of afatinib was not affected. Click-ExM revealed the distribution of the azide-functionalized afatinib (Az-afatinib) in HeLa cells, and plasma membrane blebbing during afatinib-induced cell apoptosis was observed (Fig. 4e and Extended Data Fig. 9a–c). Puromycin is an aminonucleoside antibiotic that terminates protein synthesis by covalent conjugation with nascent polypeptide chains. Here, an alkyne-containing puromycin analog, *O*-propargyl-puromycin[38] (OP-Puro), was used for click-ExM. Intense labeling was observed in various cytoplasmic foci, which probably resulted from rapid degradation of misfolded peptides by proteasome (Fig. 4f and Extended Data Fig. 9d–f). The widely used DNA stain Hoechst 33258 was derivatized with an alkyne, with which the nuclei were visualized with AF488 by click-ExM (Fig. 4g and Extended Data Fig. 9g–j). The click-ExM observed distribution of small molecules were confirmed by conventional super-resolution microscopies (Supplementary Note 1).

Two-color click-ExM. Finally, we demonstrated two-color click-ExM. Lipids and proteins in COS-7 cells were simultaneously labeled with Alk-Cho and AHA, respectively. After sequential click reactions with azide-biotin and alkyne-TAMRA, two-color click-ExM revealed the distributions of Cho-containing phospholipids and nascent proteins (Extended Data Fig. 10a). By pairing azide-biotin/streptavidin with alkyne-digoxigenin (DIG)/anti-DIG antibody, we demonstrated two-color click-ExM imaging of lipids and glycans (Extended Data Fig. 10b). Similarly, azide-FLAG/anti-FLAG antibody was used for two-color click-ExM imaging of glycans and DNA (Extended Data Fig. 10c).

Discussion

ExM has emerged as an attractive approach to perform super-resolution imaging using conventional microscopes. Click-ExM developed in this work provides a unified and convenient protocol for nanoscale imaging of any biomolecule that can be labeled with click chemistry, thus expanding the applicability of ExM to molecules not being imaged before, such as lipids and glycans. Of note, developing ExM protocols compatible with lipid imaging is currently a direction of great interest[39]. Click-ExM exploits the click-labeling method, which is applicable for various biomolecules and is advancing rapidly. By converting the click labels to streptavidin-dye conjugates, click-ExM adapts the well-established proExM workflow (a more detailed discussion is included in Supplementary Note 1). Furthermore, click-ExM is compatible with various signal-amplification techniques. In addition, click-ExM is compatible with multicolor imaging, and a promising future direction is to integrate different click reactions to enable visualization of more than two kinds of biomolecules in the same sample.

Online content

Any methods, additional references, Nature Research reporting summaries, source data, extended data, supplementary information, acknowledgements, peer review information; details of author contributions and competing interests; and statements of data and code availability are available at https://doi.org/10.1038/s41592-020-01005-2.

Received: 11 December 2019; Accepted: 28 October 2020;
Published online: 07 December 2020

References

1. Wassie, A. T., Zhao, Y. & Boyden, E. S. Expansion microscopy: principles and uses in biological research. *Nat. Methods* **16**, 33–41 (2019).
2. Chen, F., Tillberg, P. W. & Boyden, E. S. Expansion microscopy. *Science* **347**, 543–548 (2015).
3. Chen, F. et al. Nanoscale imaging of RNA with expansion microscopy. *Nat. Methods* **13**, 679–684 (2016).
4. Tillberg, P. W. et al. Protein-retention expansion microscopy of cells and tissues labeled using standard fluorescent proteins and antibodies. *Nat. Biotechnol.* **34**, 987–992 (2016).
5. Chozinski, T. J. et al. Expansion microscopy with conventional antibodies and fluorescent proteins. *Nat. Methods* **13**, 485–488 (2016).
6. Ku, T. et al. Multiplexed and scalable super-resolution imaging of three-dimensional protein localization in size-adjustable tissues. *Nat. Biotechnol.* **34**, 973–981 (2016).
7. Grammel, M. & Hang, H. C. Chemical reporters for biological discovery. *Nat. Chem. Biol.* **9**, 475–484 (2013).
8. Rostovtsev, V. V., Green, L. G., Fokin, V. V. & Sharpless, K. B. A stepwise huisgen cycloaddition process: copper(I)-catalyzed regioselective 'ligation' of azides and terminal alkynes. *Angew. Chem. Int. Ed.* **41**, 2596–2599 (2002).
9. Besanceney-Webler, C. et al. Increasing the efficacy of bioorthogonal click reactions for bioconjugation: a comparative study. *Angew. Chem. Int. Ed.* **50**, 8051–8056 (2011).
10. Agard, N. J., Prescher, J. A. & Bertozzi, C. R. A strain-promoted [3+2] azide-alkyne cycloaddition for covalent modification of biomolecules in living systems. *J. Am. Chem. Soc.* **126**, 15046–15047 (2004).
11. Lang, K. & Chin, J. W. Cellular incorporation of unnatural amino acids and bioorthogonal labeling of proteins. *Chem. Rev.* **114**, 4764–4806 (2014).
12. Jao, C. Y. et al. Metabolic labeling and direct imaging of choline phospholipids in vivo. *Proc. Natl Acad. Sci. USA* **106**, 15332–15337 (2009).
13. Martin, B. R. & Cravatt, B. F. Large-scale profiling of protein palmitoylation in mammalian cells. *Nat. Methods* **6**, 135–138 (2009).
14. Charron, G. et al. Robust fluorescent detection of protein fatty-acylation with chemical reporters. *J. Am. Chem. Soc.* **131**, 4967–4975 (2009).
15. Hannoush, R. N. & Arenas-Ramirez, N. Imaging the lipidome: ω-alkynyl fatty acids for detection and cellular visualization of lipid-modified proteins. *ACS Chem. Biol.* **4**, 581–587 (2009).
16. Charron, G., Tsou, L. K., Maguire, W., Yount, J. S. & Hang, H. C. Alkynyl-farnesol reporters for detection of protein *S*-prenylation in cells. *Mol. Biosyst.* **7**, 67–73 (2011).
17. Chen, Y. et al. Chemoproteomic profiling of targets of lipid-derived electrophiles by bioorthogonal aminooxy probe. *Redox Biol.* **12**, 712–718 (2017).
18. Lin, R. et al. A hybridization-chain-reaction-based method for amplifying immunosignals. *Nat. Methods* **546**, 275–278 (2018).
19. Luchansky, S. J., Goon, S. & Bertozzi, C. R. Expanding the diversity of unnatural cell-surface sialic acids. *ChemBioChem* **5**, 371–374 (2004).
20. Saxon, E. & Bertozzi, C. R. Cell surface engineering by a modified Staudinger reaction. *Science* **287**, 2007–2010 (2000).
21. Qin, W. et al. Artificial cysteine S-glycosylation induced by per-*O*-acetylated unnatural monosaccharides during metabolic glycan labeling. *Angew. Chem. Int. Ed.* **57**, 1817–1820 (2018).
22. Qin, K., Zhang, H., Zhao, Z. & Chen, X. Protein S-glyco-modification through an elimination-addition mechanism. *J. Am. Chem. Soc.* **142**, 9382–9388 (2020).
23. Letschert, S. et al. Super-resolution imaging of plasma membrane glycans. *Angew. Chem. Int. Ed.* **53**, 10921–10924 (2014).
24. Jiang, H. et al. Tracking surface glycans on live cancer cells with single-molecule sensitivity. *Angew. Chem. Int. Ed.* **54**, 1765–1769 (2015).
25. Möckl, L. et al. Quantitative super-resolution microscopy of the mammalian glycocalyx. *Developmental Cell* **50**, 57–72 (2019).

26. Rong, J. et al. Glycan imaging in intact rat hearts and glycoproteomic analysis reveal the upregulation of sialylation during cardiac hypertrophy. *J. Am. Chem. Soc.* **136**, 17468–17476 (2014).
27. Yang, X. & Qian, K. Protein O-GlcNAcylation: emerging mechanisms and functions. *Nat. Rev. Mol. Cell Biol.* **18**, 452–465 (2017).
28. Boyce, M. et al. Metabolic cross-talk allows labeling of O-linked β-*N*-acetylglucosamine-modified proteins via the *N*-acetylgalactosamine salvage pathway. *Proc. Natl Acad. Sci. USA* **108**, 3141–3146 (2011).
29. Woo, C. M., Iavarone, A. T., Spiciarich, D. R., Palaniappan, K. K. & Bertozzi, C. R. Isotope-targeted glycoproteomics (IsoTaG): a mass-independent platform for intact *N*- and *O*-glycopeptide discovery and analysis. *Nat. Methods* **12**, 561–567 (2015).
30. Thevathasan, J. V. et al. Nuclear pores as versatile reference standards for quantitative superresolution microscopy. *Nat. Methods* **16**, 1045–1053 (2019).
31. Clark, P. M. et al. Direct in-gel fluorescence detection and cellular imaging of O-GlcNAc-modified proteins. *J. Am. Chem. Soc.* **130**, 11576–11577 (2008).
32. Zheng, T. et al. Tracking *N*-acetyllactosamine on cell-surface glycans in vivo. *Angew. Chem. Int. Ed.* **50**, 4113–4118 (2011).
33. Dieterich, D. C. et al. In situ visualization and dynamics of newly synthesized proteins in rat hippocampal neurons. *Nat. Neurosci.* **13**, 897–905 (2010).
34. Li, J. et al. Ligand-free palladium-mediated site-specific protein labeling inside gram-negative bacterial pathogens. *J. Am. Chem. Soc.* **135**, 7330–7338 (2013).
35. Salic, A. & Mitchison, T. J. A chemical method for fast and sensitive detection of DNA synthesis in vivo. *Proc. Natl Acad. Sci. USA* **105**, 2415–2420 (2008).
36. Jao, C. Y. & Salic, A. Exploring RNA transcription and turnover in vivo by using click chemistry. *Proc. Natl Acad. Sci. USA* **105**, 15779–15784 (2008).
37. Sequist, L. V. et al. Phase III study of afatinib or cisplatin plus pemetrexed in patients with metastatic lung adenocarcinoma with EGFR mutations. *J. Clin. Oncol.* **31**, 3327–3334 (2013).
38. Liu, J. et al. Imaging protein synthesis in cells and tissues with an alkyne analog of puromycin. *Proc. Natl Acad. Sci. USA* **109**, 413–418 (2012).
39. Karagiannis, E. D. et al. Expansion microscopy of lipid membranes. Preprint at *bioRxiv* https://doi.org/10.1101/829903 (2019).

Methods

A step-by-step protocol is available as a Supplementary Protocol and an open resource in Protocol Exchange[40].

Reagents and antibodies. All reagents and antibodies were obtained from commercial suppliers, and used without further purification. Detailed information is shown in Supplementary Table 1.

Compound synthesis. Alk-Cho[12], Alk-farnesol[16], SiaNAz[19], ManNAz[20] and OP-Puro[38] were synthesized as previously described. AOyne[17] and PenK (N^{ε}-pent-4-ynyloxy-carbonyl-L-lysine)[34] were gifts from C. Wang and P.R. Chen at Peking University, respectively. The synthesis of biotin trimer, Alk-Hoechst and Az-afatinib is described in Supplementary Note 2.

Cell culture. HeLa (ATCC, CCL-2), Chinese hamster ovary (CHO) (ATCC, CCL-61), human embryonic kidney 293T (HEK293T) (ATCC, CRL-11268), U2OS (3111C0001CCC000028, National Infrastructure of Cell Line Resource, Beijing, China) and COS-7 (Cell Bank, Chinese Academy of Science, Shanghai, China) cells were cultured in Dulbecco's modified Eagle's medium (DMEM) supplemented with 10% (v/v) fetal bovine serum (FBS), 100 units ml^{-1} penicillin and 100 $\mu g\,ml^{-1}$ of streptomycin at 37 °C in a 5% (v/v) CO_2 atmosphere. Cells were used with passage numbers below 20 and free of mycoplasma contamination. The COS-7 cells expressing organelle-specific markers were generated by transient transfection with the plasmids encoded Sec61β-GFP, b4Gal-T1-GFP (a gift from L. Chen at Peking University) or mito-GFP (a gift from P. Zou at Peking University).

Animals. Wild-type Sprague-Dawley rats and C57BL/6N mice were purchased from Vital River Laboratory Animal Center and kept under specific-pathogen-free conditions. Animals were housed in the temperature-controlled animal room (around 24 °C, humidity 50–60%) with a 12-h light/12-h dark cycle. All animal experiments were performed in accordance with guidelines approved by the Institutional Animal Care and Use Committee of Peking University accredited by AAALAC International.

Cardiomyocyte isolation and culture. Single ventricular cardiomyocytes were isolated from adult rats (about 2 months old, 200–250 g). Briefly, the rats were anesthetized by 5% (v/v) isoflurane. The hearts were rapidly excised and rinsed in cold Tyrode's solution (120 mM NaCl, 4 mM KCl, 1.2 mM $MgCl_2$, 1.2 mM NaH_2PO_4, 20 mM $NaHCO_3$, 10 mM glucose and 30 mM taurine, pH 7.3–7.4). After cannulating the aorta to the Langendorff apparatus, the hearts were perfused with Tyrode's solution at 37 °C to clean the blood in vessels. The hearts were perfused to be digested in Tyrode's solution containing 10 mM taurine, 0.714 mg ml^{-1} of type II collagenase, 0.028 mg ml^{-1} of protease type XIV and 1 mg ml^{-1} bovine serum albumin (BSA). When turning soft (that is, about 40 min), the hearts were cut into small chunks in Tyrode's solution containing 10 mM taurine, 0.714 mg ml^{-1} of type II collagenase and 1 mg ml^{-1} of BSA. Single cells were then collected and resuspended with Tyrode's solution containing 10 mM taurine and 1 mg ml^{-1} of BSA, and the $CaCl_2$ concentration was restored gradually from 0.125 to 0.5 mM. The isolated cardiomyocytes were kept in Tyrode's solution (140 mM NaCl, 4 mM KCl, 1 mM $CaCl_2$, 1.2 mM $MgCl_2$, 1.2 mM NaH_2PO_4, 10 mM glucose, 10 mM HEPES, 30 mM taurine and 1 mg ml^{-1} of BSA, pH 7.3–7.4). Finally, the freshly isolated cardiomyocytes were plated on LabTek II chamber slides (NUNC, 154534) coated with 2 $\mu g\,ml^{-1}$ laminin in PBS for 10 min and the attached cells were cultured in M199 medium (supplemented with 5 mM creatine, 2 mM L-carnitine, 5 mM taurine, 25 mM HEPES, 26 mM $NaHCO_3$ and 1% (v/v) penicillin-streptomycin, pH 7.2).

Neuron isolation and culture. Hippocampal and cortical neurons were dissociated from postnatal day 0 rat pups. Briefly, the hippocampus and cortex were dissected from the brain and triturated using a pipette after trypsinization (0.25% (w/v) trypsin-EDTA at 37 °C, 7 min for the cortex and 14 min for the hippocampus). The cells were seeded on 15-mm poly-D-lysine-coated coverslips in 24-well plates and cultured in Neurobasal medium supplemented with 2% (v/v) B-27 supplement, 0.5 mM GlutaMAX, 100 u ml^{-1} of penicillin and 100 $\mu g\,ml^{-1}$ of streptomycin. One day after plating, 4 μM Ara-C was added to the cultures. The cultures were maintained at 37 °C in 5% (v/v) CO_2 atmosphere, and one-half of medium was replaced with fresh culture medium every 3–4 d.

Preparation of acute brain slices. Mice (postnatal days 21–27) were anesthetized with 5% (v/v) isoflurane and rapidly decapitated. The brain tissues were quickly removed and sliced on a vibratome (VT1200s, Leica) in ice-cold cutting solution (125 mM NaCl, 2.5 mM KCl, 26 mM $NaHCO_3$, 1.25 mM NaH_2PO_4, 1 mM $MgCl_2$, 2 mM $CaCl_2$ and 20 mM glucose, pH 7.3–7.4, saturated with 95% (v/v) O_2 and 5% (v/v) CO_2). The slices with a thickness of roughly 150 μm were then explanted on a culture membrane (Millicell CM, pore size 0.4 μm, Millipore) in a 35-mm petri dish for further labeling experiments.

Stoichiometric quantification of the streptavidin-AcX reaction. A volume of 10 μl of streptavidin at 1 mg ml^{-1} was incubated with 2 μl of 10 mg ml^{-1} AcX in PBS overnight at room temperature. The resulting AcX-modified streptavidin was analyzed on a matrix-assisted laser desorption/ionization–tandem time of flight mass spectrometer (AB Sciex 5800).

Proteinase K sensitivity of streptavidin. Streptavidin (100 μg) was incubated with proteinase K (8 u ml^{-1}) in the presence or absence of biotin (600 μM) in digestion buffer (50 mM Tris pH 8.0, 1 mM EDTA, 0.1% (v/v) Triton X-100 and 0.8 M guanidine HCl) at 37 °C for 0 h, 2 h, 4 h, or overnight at room temperature, followed by precipitation with 150 μl of methanol, 37.5 μl of chloroform and 100 μl of water. The mixtures were centrifuged at 18,000*g* for 5 min for removal of the aqueous phase, followed by addition of 100 μl of methanol. After centrifugation and removal of methanol, the precipitates were resuspended in 50 μl 1% (w/v) SDS, boiled and resolved on 12% SDS–PAGE and stained by Commassie Brilliant Blue.

Immunostaining. The cells were fixed with 3% (w/v) formaldehyde and 0.1% (v/v) GA in PBS for 15 min and reduced with 0.1% (w/v) sodium borohydride for 7 min. After washing three times with 100 mM glycine in PBS, cells were permeabilized with 0.1% (v/v) Triton X-100 in PBS for 15 min. Cells were blocked in blocking buffer (1× PBS/5% (w/v) BSA/0.1% (v/v) Tween 20) for 30 min, and incubated with primary antibody in antibody dilution buffer (1× PBS/1% (w/v) BSA/0.1% (v/v) Tween 20) overnight at 4 °C, then cells were washed three times with PBS and incubated with fluorophore-conjugated secondary antibody in antibody dilution buffer for 1 h and washed three times with PBS. Specifically, for α-tubulin immunostaining, a cytoskeleton extraction step was performed before fixing the cells. Briefly, the cells were extracted in cytoskeleton extraction buffer (0.2% (v/v) Triton X-100, 0.1 M PIPES, 1 mM EGTA and 1 mM $MgCl_2$, pH 7.0) for 1 min at room temperature. For Tom20 immunostaining in Fig. 2b and Extended Data Fig. 3a, COS-7 cells were incubated with primary antibody in antibody dilution buffer (1× PBS/1% (w/v) BSA/0.1% (w/v) saponin) before the ExM procedure, and AF647-conjugated secondary antibody was then incubated with gel overnight in antibody dilution buffer at 4 °C after gelation and digestion step.

Metabolic labeling of lipids. COS-7 and HeLa cells were incubated with 100 or 200 μM Alk-Cho for 12 h, 200 μM Alk-palmitic acid for 24 h, 200 μM Alk-myristic acid for 24 h, 200 μM Alk-stearic acid for 12 h or 100 μM Alk-farnesol for 24 h. The lipid reporters were dissolved in medium, which was vortexed vigorously before added to cells. For HNE labeling, cells were incubated with 50 μM HNE in medium for 1 h, washed with warm medium for 30 min, and incubated with 1 mM AOyne for 30 min. All the cells were then fixed with 3% (w/v) formaldehyde and 0.1% (v/v) GA in PBS for 15 min and reduced with 0.1% (w/v) sodium borohydride for 7 min. After washing three times with 100 mM glycine in PBS, the cells were permeabilized with 0.1% (w/v) saponin in PBS for 5 min and washed three times with PBS. The cells were incubated with 50 μM azide-PEG_3-biotin, BTTAA-$CuSO_4$ complex (50 μM $CuSO_4$, BTTAA/$CuSO_4$ 6:1, mol/mol) and 2.5 mM sodium ascorbate in PBS at room temperature for 1 h, followed by five washes with PBS. The cells were then incubated with 5 $\mu g\,ml^{-1}$ of streptavidin-dye conjugates in PBS containing 1% (w/v) BSA for 1 h, and washed three times with PBS. The labeled cells were immediately proceeded to the next step to avoid potential signal loss or distortion.

Metabolic labeling of glycans. For O-GlcNAc labeling, HeLa and CHO cells were incubated with 1 mM GalNAz for 48 h. The cells were fixed with 4% (w/v) formaldehyde in PBS for 15 min, washed three times with PBS and permeabilized with 0.1% (v/v) Triton X-100 in PBS for 15 min. After three washes with PBS, the cells were incubated with 50 μM alkyne-PEG_4-biotin, BTTAA-$CuSO_4$ complex (50 μM $CuSO_4$, BTTAA/$CuSO_4$ 6:1, mol/mol) and 2.5 mM sodium ascorbate in PBS at room temperature for 1 h, followed by five washes with 0.1% (v/v) Tween 20 in PBS. For sialoglycan labeling, HeLa cells, rat hippocampus neurons and rat cardiomyocytes were incubated with 2 mM SiaNAz or ManNAz for 48 h. After three washes with warm medium, the cells were incubated with 100 μM DBCO-biotin in medium at 37 °C for 30 min and then washed with warm medium for 15 min. The cells were then fixed with 3% (w/v) formaldehyde and 0.1% (v/v) GA in PBS for 15 min, reduced with 0.1% (w/v) sodium borohydride for 7 min and washed three times with 100 mM glycine in PBS. For samples where immunostaining was performed, the cells were permeabilized with 0.1% (w/v) saponin in PBS for 5 min and washed three times. The cells were then incubated with 5 $\mu g\,ml^{-1}$ of streptavidin-dye conjugates in PBS containing 1% (w/v) BSA for 1 h and washed three times with PBS. For ManNAz-labeled rat cardiomyocytes, isHCR was performed for signal amplification (detailed procedures described below).

Chemoenzymatic labeling of glycans. For O-GlcNAc labeling, CHO cells were fixed and permeabilized as described in the GalNAz labeling experiments, followed by incubation in the labeling solution containing 25 $\mu g\,ml^{-1}$ of Y289L GalT1, 500 μM UDP-GalNAz, 1 mM $MnCl_2$, 50 mM NaCl, 20 mM HEPES (pH 7.9) and 2% (v/v) Nonidet P40 at 4 °C for 20 h. After five washes with PBS, the cells were labeled as described in the GalNAz labeling experiments. For LacNAc labeling, HeLa cells were washed three times with PBS and incubated in the labeling solution containing 20 mM $MgSO_4$, 3 mM HEPES, 1% (v/v) FBS, 500 μM GDP-FucAz and

50 μg ml^{-1} α1,3-FucT (a gift from J. Li at Nanjing University) at 37 °C for 15 min. After three washes with PBS, the cells were labeled by incubation with 50 μM alkyne-PEG$_4$-biotin, BTTAA-CuSO$_4$ complex (50 μM CuSO$_4$, BTTAA/CuSO$_4$ 6:1, mol/mol) and 2.5 mM sodium ascorbate in PBS for 10 min, and fixed with the same procedures as described in the SiaNAz or ManNAz labeling experiments. Iterative biotin trimer-streptavidin staining was performed for signal amplification (detailed procedures described below).

Metabolic labeling of proteins. The cells were incubated with 2 mM AHA for 1 h (for rat cortical neurons and U2OS cells) or 1 mM AHA for 18 h (for HeLa cells). After three washes with PBS, the cells were fixed, permeabilized and labeled with the same procedures as described in the GalNAz labeling experiments.

Site-specific labeling of proteins. To the plasmid encoding a protein of interest bearing the amber codon (pCDNA3.1-GFP-Y40TAG, pCMV3-KRAS-G21V-I21TAG (a gift from P. R. Chen at Peking University), or pEGFP-H2B-V112TAG) mixed with the plasmid encoding PenK-MbPylRS-tRNA$^{Pyl}_{CUA}$ (CUA, the anticodon of the amber codon; Pyl, pyrrolysine; a gift from P. R. Chen at Peking University) in Opti-MEM (plasmid ratio 1:1) was added X-tremeGENE HP (Roche) at the ratio of 500 ng total plasmids to 1 μl X-tremeGENE HP. The solution was incubated for 15 min and applied to HEK293T or COS-7 cells grown on poly-D-lysine-coated eight-well glass chamber slides (Nunc, 154534) with around 60% confluence. After the cells were cultured for 6 h, the cell culture medium was changed to fresh medium supplemented with 200 μM PenK and the cells were further grown for 24 h. After washing three times with fresh medium (1 h each), the cells were fixed and permeabilized as described in the lipid labeling experiments (for the KRas-expressing cells) or as described in the GalNAz labeling experiments (for the GFP- and H2B-expressing cells). The cells were then click-labeled with azide-PEG$_3$-biotin and stained with streptavidin-dye conjugates.

Metabolic labeling of nucleic acids. For DNA labeling, the cells were incubated with 10 μM EdU for 24 h (for U2OS cells) or 100 μM EdU for 12 h (for HeLa cells). For nascent DNA labeling in the S phase, U2OS cells were labeled with 10 μM EdU for varied durations of time ranging from 15 min to 1 h. For RNA labeling, HeLa cells were labeled with 1 mM EU for 4 h. All the cells were fixed with 4% (w/v) formaldehyde in PBS for 15 min. After three washes with PBS, the cells were permeabilized with 0.1% (v/v) Triton X-100 in PBS for 15 min. The cells were incubated with 100 μM azide-PEG$_3$-biotin, 500 μM CuSO$_4$, 2 mM THPTA and 5 mM sodium ascorbate in PBS at room temperature for 1 h, followed by five washes with PBS. The cells were incubated with 5 μg ml^{-1} of streptavidin-dye conjugates in PBS containing 1% (w/v) BSA for 1 h and washed three times with PBS.

Labeling of small molecules. HeLa cells were treated with 10 μM Az-afatinib in DMEM for 12 h. After three washes with PBS, the cells were fixed and permeabilized as described in the lipid labeling experiments and labeled as described in the GalNAz labeling experiments.

For OP-Puro, HeLa cells were treated with 50 μM OP-Puro in DMEM for 2 h. After washing with warm DMEM for 15 min, the cells were fixed, permeabilized as described in the GalNAz labeling experiments and labeled as described in the lipid labeling experiments.

For Alk-Hoechst, HeLa cells were treated with 0.5–20 μM Alk-Hoechst for 45 min and washed three times with warm DMEM for 1 h, followed by labeling using the same procedures as described in the nucleic acid labeling experiments.

Gelation, digestion and expansion. ExM was performed as previously described with some modifications[4,5]. For anchoring with AcX, the cells are incubated in 0.1 mg ml^{-1} of AcX in PBS overnight at room temperature, followed by washing three times with PBS. For anchoring with GA, the cells are incubated with 0.25% (v/v) GA in PBS for 10 min, followed by washing three times with PBS. The monomer solution (1× PBS, 2 M NaCl, 2.5% (w/v) acrylamide, 0.15% (w/v) *N*,*N*′-methylenebisacrylamide and 8.625% (w/v) sodium acrylate) was prepared, frozen in aliquots and thawed before use. Freshly prepared 10% (w/w) *N*,*N*,*N*′,*N*′-tetramethylethylenediamine (TEMED) and 10% (w/w) ammonium persulfate (APS) were diluted in monomer solution to a final concentration of 0.2% (w/w) to give the gelation solution. The cells were incubated with the gelation solution at 4 °C for 5 min, and then transferred to a humidified 37 °C incubator for 1 h for gelation. The hydrogel was digested in the digestion buffer (50 mM Tris, 1 mM EDTA, 0.1% (v/v) Triton X-100 and 0.8 M guanidine HCl, pH 8.0) containing 8 u ml^{-1} proteinase K at 37 °C for 4 h for AcX-anchored samples or 2 h for GA-anchored samples. The hydrogel was transferred to deionized water to expand. Water was changed every 20 min until the expansion process was completed. The nuclei were stained with 5 μg ml^{-1} of Hoechst 33342 to facilitate locating the cells in the hydrogel.

isHCR amplification. isHCR amplification was performed as previously described with some modifications[18]. A pair of DNA-fluorophore HCR amplifiers (100 μM each) in 5× SSC buffer were separately snap-cooled at 95 °C for 90 s and then left at room temperature over 30 min. The streptavidin-dye-stained cells were incubated with 0.5 μM DNA-biotin HCR initiator at room temperature for 1 h. The cells were then washed five times with PBS and incubated in amplification buffer (5× SSC buffer, 0.1% (v/v) Tween 20 and 10% (w/v) dextran sulfate in ddH_2O) containing the pair of DNA-fluorophore HCR amplifiers (150 nM each) overnight at room temperature, followed by five washes with PBS.

The sequences of DNA-fluorophore HCR amplifiers and DNA-biotin HCR initiator:

B1 Amplifier H1: 5′-AF546-CGTAAAGGAAGACTCTTCCCGTTTGCTGCCCTCCTCGCA
TTCTTTCTTGAGGAGGGCAGCAAACGGGAAGAG-3′
B1 Amplifier H2: 5′-GAGGAGGGCAGCAAACGGGAAGAGTCTTCCTTTACGCTCTTCC
CGTTTGCTGCCCTCCTCAAGAAAGAATGC-AF546-3′
B1I2: 5′-Acrydite-ATATAGCATTCTTTCTTGAGGAGGGCAGCAAACGGGAAGAG-Biotin-3′

Biotin trimer amplification. The cells stained with streptavidin-dye conjugates were incubated with 50 μM biotin trimer at room temperature for 30 min and washed five times with PBS. The cells were then incubated with 5 μg ml^{-1} of streptavidin-dye conjugates in PBS containing 1% (w/v) BSA for 30 min, and washed five times with PBS. This cycle was repeated for four times for LacNAc-labeled cells. The cycle number can be adjusted to achieve desired amplification.

Labeling of acute brain slices. For Alk-Cho labeling, the slices were incubated in slice culture medium (Neurobasal Plus medium, 2% (v/v) GlutaMAX, 1% (v/v) B-27 supplement and 1% (v/v) penicillin-streptomycin-glutamine) containing 1.5 mM Alk-Cho at 37 °C for 6 h. For AHA labeling, the slices were incubated in artificial cerebrospinal fluid (125 mM NaCl, 2.5 mM KCl, 2 mM $CaCl_2$, 1 mM $MgCl_2$, 1.25 mM NaH_2PO_4, 25 mM $NaHCO_3$ and 11 mM glucose, pH 7.3–7.4) containing with 4 mM AHA at room temperature for 4 h. All slices were rinsed twice with PBS, fixed with 4% (w/v) paraformaldehyde in PBS at 4 °C for 12 h and stored temporarily in 30% (w/v) sucrose at 4 °C. The slices were washed with 100 mM glycine for 1 h, and permeabilized for 30 min with 0.1% (w/v) saponin in PBS for the Alk-Cho-labeled slices or 0.1% (v/v) Triton X-100 in PBS for the AHA-labeled slices. The slices were then incubated with corresponding click-labeling reagents overnight at 4 °C and washed three times (1 h each) with 0.1% (w/v) saponin for the Alk-Cho-labeled slices or 0.1% (v/v) Tween 20 for the AHA-labeled slices. All the slices were incubated with 5 μg ml^{-1} of streptavidin-dye conjugates in 0.1% (w/v) saponin or 0.1% (v/v) Tween 20 overnight at 4 °C, stained with 5 μg ml^{-1} of Hoechst 33342 and washed three times with PBS (1 h each).

Gelation, digestion and expansion of mouse brain slices. The brain slices were treated with 0.1 mg ml^{-1} of AcX in a 2-(*N*-morpholino)ethanesulfonic acid (MES)-buffered saline (100 mM MES and 150 mM NaCl, pH 6.0) for 24 h at room temperature, followed by three washes with PBS. The gelation solution for brain slices was the same as the one for cell samples except for the addition of 0.01% (w/w) 4-hydroxy-TEMPO from a 0.5% (w/w) stock as an inhibitor for polymerization. The brain slices were incubated in gelation solution for 1 h at 4 °C before gelation. The gelation chamber was constructed by placing two stacks of three pieces of no. 1.5 coverglass (high-precision, Fisher Scientific) on a glass slide. The samples were allowed to gel in fresh gelation solution for 2.5 h at 37 °C. Excess gel around the samples was trimmed off by a razor blade, and the samples were digested in digestion buffer with 8 u ml^{-1} of Proteinase K overnight at room temperature or for 6 h at 37 °C. The hydrogel was transferred into deionized water to expand. The nuclei were stained with 5 μg ml^{-1} of Hoechst 33342.

Two-color click-ExM imaging. For two-color imaging of lipids and proteins, COS-7 cells were simultaneously treated with 100 μM Alk-Cho and 1 mM AHA for 12 h. The cells were fixed and permeabilized as described in the lipid labeling experiments. The cells were reacted with azide-PEG$_3$-biotin and stained with streptavidin-AF488. After washing three times with 0.1% (w/v) saponin in PBS, the cells were postfixed with 4% (w/v) formaldehyde in PBS for 10 min. The cells were then reacted with alkyne-TAMRA, followed by three washes with 0.2% (v/v) Tween 20 in PBS.

For two-color imaging of lipids and glycans, COS-7 cells incubated with 2 mM ManNAz for 36 h, to which 100 μM Alk-Cho was added. The cells were incubated for another 12 h. After three washes with PBS, the cells were click-labeled with alkyne-DIG at room temperature for 10 min and washed with PBS. The cells were fixed and permeabilized as described in the lipid labeling experiments. The cells were reacted with azide-PEG$_3$-biotin and stained with streptavidin-AF555. After postfixing with 4% (w/v) formaldehyde in PBS for 10 min, the cells were immunostained with DyLight 488-conjugated anti-DIG antibody. The cells were washed three times with 0.2% (v/v) Tween 20 in PBS.

For two-color imaging of glycans and DNA, HeLa cells were incubated with 1 mM GalNAz for 24 h, to which 10 μM EdU was added. The cells were incubated for another 24 h. The cells were fixed and permeabilized as described in the

GalNAz labeling experiments. The cells were reacted with alkyne-PEG$_4$-biotin and stained with streptavidin-AF488. After five washes with 0.2% (v/v) Tween 20 in PBS, the cells were reacted with azide-FLAG and immunostained with anti-FLAG primary antibody and AF555-conjugated secondary antibody. The cells were washed three times with 0.2% (v/v) Tween 20 in PBS.

Quantification of fluorescence retention during click-ExM. Epifluorescence images of the click-labeled cells were acquired on a Nikon Eclipse Ts2R-FL inverted microscope. Following AcX treatment, click-ExM gelation and digestion, the samples were washed three times with digestion buffer (without Proteinase K). The epifluorescence images were taken again on the same cell regions with identical imaging conditions. For intensity measurements on each sample before and after processing, the same cell regions were segmented and integrated intensity was measured to account for fluorophore dilution.

Microscopy. Imaging acquisition was performed within 24 h after expansion for all samples. To minimize drift of expanded samples during data acquisition, 24 × 50 mm rectangular no. 1.5 coverglass was coated with 0.1 mg ml^{-1} of poly-D-lysine for 10 min at room temperature and allowed to dry. Excess water was carefully removed using laboratory wipes, and expanded samples were stably attached to the glass surface and maintained immobile during data collection.

Widefield microscopy. Widefield imaging was performed using a Nikon Eclipse Ts2R-FL inverted microscope equipped with a Plan Fluor ×10/0.30-NA (numerical aperture) Ph1 DL air objective (Nikon), a ProScan III unit (Prior Scientific), 390/38 and 470/40-nm excitation filters (Chroma Technology) and a CoolSNAP DYNO camera (Photometrics), which were controlled by the NIS-Elements BR software.

Confocal microscopy. Confocal imaging was mainly performed on a Leica SP8X laser scanning confocal system with a HC PL APO CS2 ×63/1.40-NA oil-immersion objective. An HC PL APO CS2 ×40/1.30-NA oil-immersion objective was also used for imaging (Figs. 2b–j and 3c and Extended Data Figs. 3a–c,g–k (except Alk-farnesol group in 3j), 5c and 6e). HC PL APO CS2 ×10/0.40-NA air objective, HC PL APO CS2 ×20/0.75-NA air objective and HC PL APO CS2 ×40/1.10-NA water objective were used for tissue imaging (Fig. 4b and Extended Data Fig. 4). White light laser (470–670 nm) was set to 70% of maximum power, a 405-nm diode laser was used for Hoechst 33342 excitation and 488-nm and 552-nm OPSL lasers were also used for excitation. Some samples were imaged on a Zeiss LSM 700 laser scanning confocal system with a Plan-Apochromat ×63/1.40-NA DIC M27 oil-immersion objective (Extended Data Fig. 6b,d). The pinhole during all the image acquisition was opened at 1 Airy unit. Laser powers and detector gain were optimized for each sample.

Structured illumination microscopy. Lattice structured illumination microscopy imaging was performed on a Zeiss Elyra 7 with a Plan-Apochromat ×63/1.40-NA DIC M27 oil-immersion objective. The system was controlled by the ZEN software (Zeiss, black edition). AF555-labeled samples were excited using a 561-nm laser with laser powers optimized for each sample. Emission was collected through a 570–620-nm filter and a PCO edge sCMOS camera. Image processing was performed by ZEN using automatic parameters.

Airyscan microscopy. A Zeiss LSM 900 with an Airyscan 2 detector was used for image acquisition in combination with a Plan-Apochromat ×63/1.40-NA DIC M27 oil-immersion objective. The system was controlled by the ZEN software (Zeiss, blue edition). AF555-labeled samples were excited using a 561-nm laser with laser powers optimized for each sample. Emission was collected in Airyscan SR detector mode. Image processing was performed by ZEN Airyscan processing using automatic deconvolution parameters.

Stimulated emission depletion (STED) microscopy. STED imaging was performed on a Leica TCS SP8 STED 3X STED microscope with an HCX PL APO CS2 ×100/1.40-NA oil-immersion objective. The system was controlled by the LAS X software (Leica). AF488-labeled samples were excited using a 495-nm laser and a 592-nm STED laser was used for depletion. The pinhole size was set to 0.4 of an Airy unit. Laser powers were optimized for each sample. Emission was collected with a HyD detector between 505 and 581 nm.

Imaging processing and analysis. Images were mainly processed and analyzed by Fiji/ImageJ (https://fiji.sc)[41]. To improve signal visibility, images were only contrasted by changing the minimum and maximum displayed values. Maximal intensity projection of images was used in most cases. All intensity profiles were measured and normalized over a line across the region of interest. For intensity profile in Fig. 3g, the intensity data were normalized and multi-peak fitted to a Gaussian function. For full-width-at-half-maximum (FWHM) measurement in Extended Data Fig. 1e,f, intensity profiles were measured over lines perpendicular to the microtubule orientation. The data were fitted to a Gaussian function and FWHM was calculated from the Gaussian fitting. For size quantification in Fig. 3h, Fig. 3f was first segmented using automatic Otsu algorithm, and minimum Feret diameter was then measured with 'analyze particles' (size between 0.1–0.2 µm^2, postexpansion unit). The preclick-ExM image in Fig. 4d was resized to the same size of postclick-ExM image by bicubic interpolation. For intensity quantification in Supplementary Note Fig. 1b, postclick-ExM images were first matched with corresponding preclick-ExM images by cropping and rotation. The images were then segmented using automatic Otsu algorithm, and the integrated intensity was measured in the segmented areas.

The three-dimensional (3D) visualization of images was performed in Imaris (Bitplane) with MIP mode (Figs. 2h, 3b and 4b middle and right and Extended Data Figs. 4b,c and 6d). Images in Extended Data Fig. 6b were deconvolved by the Huygens software (Scientific Volume Imaging) using theoretical point spread functions and water as 'Mounting Medium'. STED images in Supplementary Note Fig. 2 were deconvolved by the Lightning adaptive approach (Leica) using theoretical point spread functions and Glycerol/Water (80:20, Refractive index 1.4429) as 'Mounting Medium'.

Statistical analysis and curve plotting were performed with Prism (GraphPad) and Origin Pro (OriginLab). Chemical structures were drawn using ChemDraw Professional (PerkinElmer). Crystal structure was visualized using PyMOL Molecular Graphics system (Schrödinger, LLC). All graphs were assembled with Adobe Illustrator.

Expansion factor calculation and distortion analysis. gEF was quantified by the sizes of the pre- and postexpanded gels: $\mathrm{gEF} = \sqrt{x_{\mathrm{EF}} \times y_{\mathrm{EF}}}$, where x_{EF} and y_{EF} are the post-/pre-ratios of gel length and width, respectively. For brain slices, the nuclei were stained using Hoechst 33342 and expansion factor was quantified by the distance of same nucleus landmarks before and after expansion with widefield microscopy equipped with low-magnified objectives.

Rigid registration and sEF calculation. Image registration and sEF calculation procedures were adapted from a previous report with some modifications[5], which were performed using MATLAB R2018a (MathWorks). The pre-expansion images were first stretched by a scaling factor (F_{esti}) of 3.8–4.8 with bicubic interpolation to approximately match the scale of the postexpansion images. This estimated expansion factor was roughly decided based on the macroscopic measurement of gel sizes. The stretched pre-expansion images were used as the 'fixed image' for rigid registration, and the postexpansion images as the 'moving image'. Rigid registration was performed using the monomodal intensity-based registration with imregtform function. Affine transformation was used in the function to correct the shear deformation of the gel. The x- and y-scaling elements (x_{corr} and y_{corr}) in the transformation matrix calculated by the imregtform function were used to correct the rough scaling factor (F_{esti}). The final expansion factor (sEF) was therefore calculated as $\mathrm{sEF} = F_{\mathrm{esti}} \times \sqrt{x_{\mathrm{corr}} \times y_{\mathrm{corr}}}$.

Nonrigid B-spline registration and distortion analysis. The registered pre- and postexpansion images were then subjected to B-spline nonrigid registration, which was adapted from a previous report with some modifications[5]. To exclude regions with no features, masks of the rigid registered pre- and postexpansion images were generated by Gaussian blur to subtract the background. The displacement field and B-spline registered images were then acquired with the imregdemons function, and the distortion vector fields were plotted with the quiver function. The r.m.s. error was quantified by calculating the difference of distance between each pair of matching features before and after B-spline registration, and plotted as a function of the distance between the matching features.

Reporting Summary. Further information on research design is available in the Nature Research Reporting Summary linked to this article.

Data availability

Source data for Figs. 2c,e,g,j and 3d,g,h and Extended Data Figs. 1c,e,f,i,j, 3f, 5c, 6h,k, 7e, 8c,h and 9c,f,j are available with this paper. All other data in this study are available from the corresponding author upon reasonable request.

Code availability

The MATLAB codes and examples for registration and distortion analysis are available from GitHub (https://github.com/Yujie-S/Click-ExM_data_process_and_example).

References

40. Sun, D. et al. Click-ExM enables expansion microscopy for all biomolecules. *Protoc. Exch.* https://doi.org/10.21203/rs.3.pex-1179/v1 (2020).
41. Schindelin, J. et al. Fiji: an open-source platform for biological-image analysis. *Nat. Methods* **9**, 676–682 (2012).

Acknowledgements

We thank S. Wang (Peking University) and Y. Rao (Peking University) for assistance on cell and tissue sample preparation, W. Zhou at the Analytical Instrumentation Center of Peking University for help on matrix-assisted laser desorption/ionization mass

spectrometry, Y. Liang (Carl Zeiss, Shanghai Co., Ltd) for help on Elyra Lattice structured illumination microscopy and LSM 900 Airyscan imaging and L. Gu for helpful discussions. This work is supported by the National Key Research and Development Projects (grant no. 2018YFA0507600 to X.C.) and the National Natural Science Foundation of China (nos. 91753206 and 21521003 to X.C.).

Author contributions

X.C. conceived the study and supervised the project. X.C. and D.S. designed the experiments and analyzed the data. D.S. conducted most of the experiments unless specified otherwise. X.F., H.Z., B.C., Q.T., W.L. and Y.Z. performed most of the chemical synthesis. J.B. synthesized Az-afatinib under the supervision of X.L. Y.S. and D.S. performed expansion factor calculation and distortion analysis. Z.H., W.L., Y.L. and X.W. prepared primary cell and tissue samples. D.S. and X.C. wrote the manuscript with input from all the authors.

Competing interests

A Chinese patent application (application no. 201911150397.1) covering the use of click-ExM has been filed in which the Peking University is the applicant, and X.C. and D.S. are the inventors.

Additional information

Extended data is available for this paper at https://doi.org/10.1038/s41592-020-01005-2.

Supplementary information is available for this paper at https://doi.org/10.1038/s41592-020-01005-2.

Correspondence and requests for materials should be addressed to X.C.

Peer review information Rita Strack was the primary editor on this article and managed its editorial process and peer review in collaboration with the rest of the editorial team.

Reprints and permissions information is available at www.nature.com/reprints.

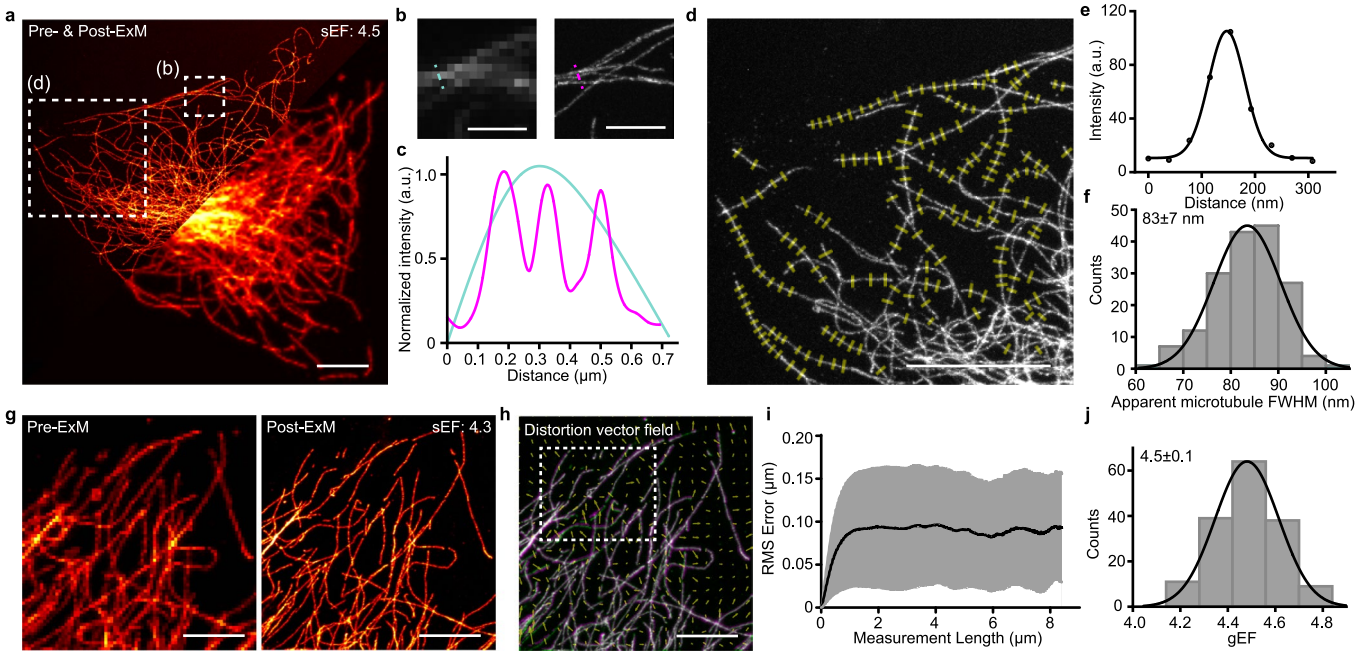

Extended Data Fig. 1 | Adaption of the protein-retention ExM (proExM) protocol for click-ExM. HeLa cells were immunostained for α-tubulin. **a**, Post-proExM image of α-tubulin (AF555, red hot, top left) partially overlaid with the corresponding pre-expansion image (bottom right). AcX was used for anchoring. sEF, expansion factor determined by transformation matrix after rigid registration. **b**, Zoomed-in view of the boxed region in **a** showing corresponding pre-proExM (left) and post-proExM (right) images of α-tubulin. **c**, Fluorescence intensity profiles along the lines in **b**. a.u., arbitrary units. **d**-**f**, Diameter of α-tubulin resolved from the zoomed-in view of the boxed region in **a**, showing the post-proExM image (**d**), a representative cross-sectional intensity profile of α-tubulin (dots) with Gaussian fitting (solid line) (**e**), and distribution of Gaussian-fitted full-width-at-half-maximum (FWHM) of the intensity profiles along yellow lines in **d**, yielding an average FWHM of 83 ± 7 nm (mean ± s.d., n = 170) (**f**). **g**-**i**, Nanoscale isotropy of proExM. Pre- and post-ExM images (**g**) were aligned using rigid registration. Post-ExM images before and after non-rigid registration were overlaid and shown in green and magenta, respectively (**h**). The yellow arrows in **h** indicate the distortion vector field. From the boxed region in **h**, the root mean square (RMS) error was quantified as a function of measured distance (**i**), in which the black line indicates mean value and the grey area indicates ± s.d. **j**, Quantification of gEF, expansion factor determined by the gel size. From 161 gels of both proExM and click-ExM experiments, an average gEF was determined to be 4.5 ± 0.1 (mean ± s.d.). Scale bars: 5 μm (**a**, **d**, **g**, **h**) and 2 μm (**b**). All distances and scale bars correspond to the pre-expansion dimensions based on sEF. Representative images from ≥3 independent experiments.

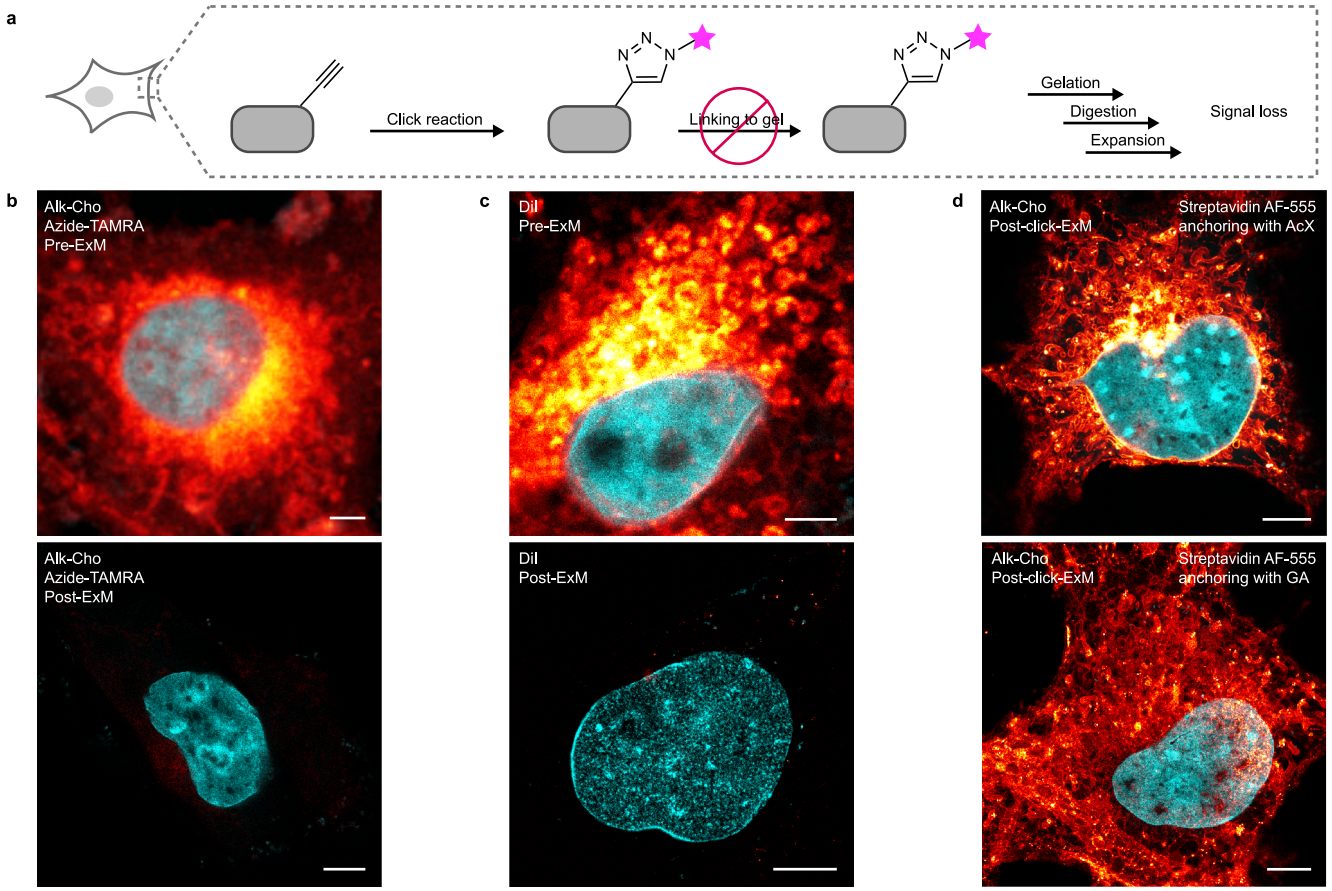

Extended Data Fig. 2 | Click-ExM preserves lipid labeling signal by streptavidin-fluorophore conjugates. a, The cells were treated with Alk-Cho to metabolically label Cho-containing phospholipids, followed by reaction with azide-dye and the standard proExM procedure. **b**, Pre- and post-ExM images of COS-7 cells treated with Alk-Cho and reacted with azide-TAMRA (red hot). **c**, Pre- and post-ExM images of COS-7 cells stained with the lipophilic dye, DiI (red hot). **d**, Click-ExM images of COS-7 cells treated with Alk-Cho, reacted with azide-biotin, and stained with SA-AF555 (red hot) was compatible with anchoring with AcX (top) and GA (bottom). The nuclei were stained by Hoechst 33342 (cyan). AcX (**b**, **c**) was used for anchoring. Scale bars: 5 μm (**b**-**d**). All distances and scale bars correspond to the pre-expansion dimensions based on gEF. Representative images from ≥3 (**d**) or 2 (**b**, **c**) independent experiments.

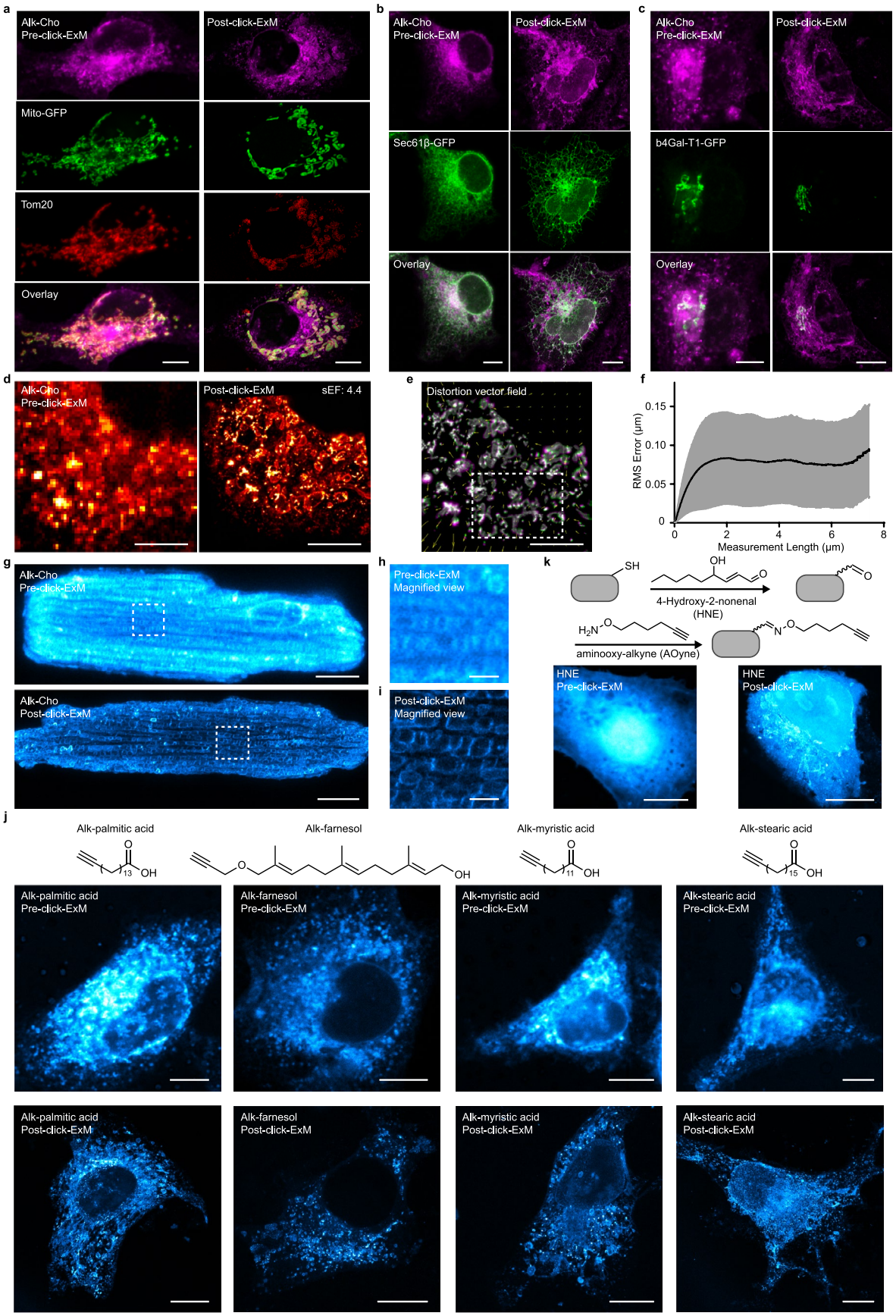

Extended Data Fig. 3 | See next page for caption.

Extended Data Fig. 3 | Pre- and post-click-ExM imaging of lipids (Related to Fig. 2). a, Pre- and post-click-ExM images of Alk-Cho-labeled phospholipids (AF555, magenta) in COS-7 cells. Mito-GFP (green) was expressed in the mitochondrial matrix and Tom20 located in the mitochondrial outer membrane was immunostained with AF647 (red). **b**, Pre- and post-click-ExM images of Alk-Cho-labeled phospholipids (AF555, magenta) and ER expressing Sec61β-GFP (green) in COS-7 cells. **c**, Pre- and post-click-ExM images of Alk-Cho-labeled phospholipids (AF555, magenta) and Golgi expressing b4Gal-T1-GFP (green) in COS-7 cells. The same post-click-ExM images were shown in Fig. 2. **d**-**f**, Nanoscale isotropy of click-ExM for imaging of Alk-Cho-labeled phospholipids. Pre- and post-click-ExM images (**d**, AF488, red hot) were aligned using rigid registration. Post-click-ExM images before and after non-rigid registration were overlaid and shown in green and magenta, respectively (**e**). The yellow arrows in **e** indicate the distortion vector field. From the boxed region in **e**, the RMS error was quantified as a function of measured distance (**f**), in which the black line indicates mean value and the grey area indicates ± s.d. **g**, Pre- and post-click-ExM images of Alk-Cho-labeled phospholipids (AF555, cyan hot) in rat cardiomyocytes. (**h**) Zoomed-in view of the boxed region from the pre-click-ExM image in **g**. **i**, Zoomed-in view of the boxed region from the post-click-ExM image in **g**. **j**, Pre- and post-click-ExM images of lipids in cells metabolically labeled with various bioorthgonal reporters including Alk-palmitic acid, Alk-farnesol, Alk-myristic acid and Alk-stearic acid (AF555, cyan hot). COS-7 cells were used for Alk-farnesol labeling and HeLa cells were used for other lipids labeling. **k**, Pre- and post-click-ExM images of 4-hydroxy-2-nonenal (HNE)-labeled protein carbonylation (AF555, cyan hot) in HeLa cells. Cysteine residues were reacted with HNE through Michael addition, reacted with aminooxy-alkyne (AOyne), and followed with the click-ExM workflow. GA (**a**-**c**, **g**-**i**) or AcX (**d**, **e**, **j**, **k**) was used for anchoring. Scale bars: 10 μm (**a**-**e**, **g**, **j**, **k**) and 2 μm (**h**, **i**). All distances and scale bars correspond to the pre-expansion dimensions based on gEF (**a**-**c**, **g**-**k**) or sEF (**d**-**f**). Analysis of isotropy from ≥3 (**d**-**f**) independent experiments. Representative images from ≥3 (**g**-**i**, pre-click-ExM images of **j**) or 2 (**a**-**c**, **k**, post-click-ExM images of **j**) independent experiments.

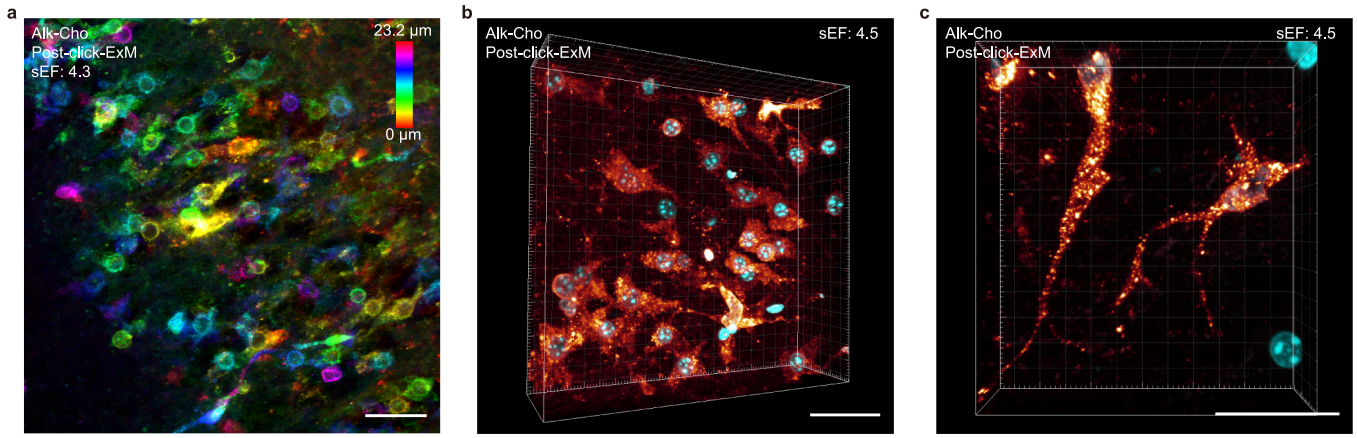

Extended Data Fig. 4 | Click-ExM imaging of Cho-containing phospholipids in the mouse brain. a–c, Acute mouse brain slices with a thickness of 150 μm were metabolically labeled with Alk-Cho. Post-click-ExM image with an imaging depth of ~23 μm (**a**) and 3D rendering images of post-click-ExM (**b**, **c**) are shown. Cho-containing phospholipids were stained with SA-AF555 in **a** and **b** or with SA-AF488 in **c**. Images were acquired using a 20×/0.75-NA air objective for **a** or a 40×/1.10-NA water objective for **b** and **c**. The nuclei were stained with Hoechst 33342 (cyan) in **b** and **c**. Scale bars: 20 μm. All distances and scale bars correspond to the pre-expansion dimensions based on sEF. Representative images from ≥3 slices.

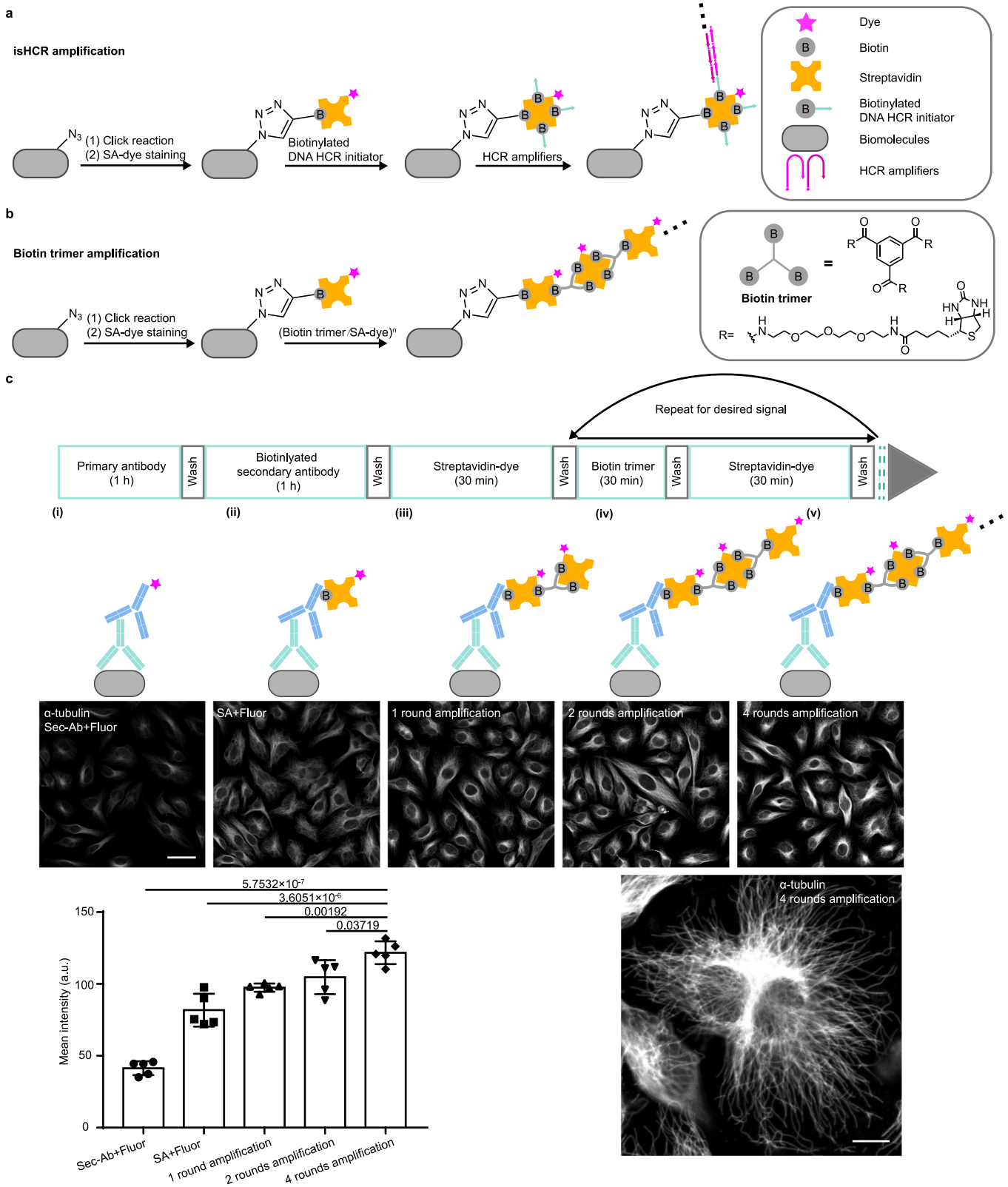

Extended Data Fig. 5 | See next page for caption.

Extended Data Fig. 5 | Signal amplification by immunosignal hybridization chain reaction (isHCR) or by a biotin trimer. a, Workflow of isHCR for signal amplification. Cells click-labeled with streptavidin-dye were incubated with DNA-biotin HCR initiators, and then incubated with a pair of DNA-fluorophore HCR amplifiers for signal amplification. **b**, Workflow of iterative signal amplification by using the biotin trimer. **c**, Fluorescence imaging of HeLa cells with α-tubulin immunostained with AF555, which was amplified by using the biotin trimer. Procedures of iterative signal amplification (top). HeLa cells were immunostained for α-tubulin, and five labeling conditions were used for comparison from left to right: (i) conventional antibody staining with AF555-conjugated secondary antibody, (ii) biotin-conjugated secondary antibody and streptavidin-AF555, (iii)-(v) one, two and four rounds of iterative staining by biotin trimer and streptavidin-AF555. Representative images of each conditions were shown (middle). Histogram shows mean fluorescence intensity quantification in five labeling conditions (n = 5 fields of view per sample, bottom left). Bars represent the mean value and error bars represent the s.d. The *P* values are listed, and $P < 0.05$ was considered significant. One-way ANOVA with post hoc Tukey HSD calculator was used for statistical analysis. Magnified image for four rounds signal amplification of immunostained α-tubulin in HeLa cells was shown (bottom right). Scale bars: 50 μm (**c**, middle) and 10 μm (**c**, bottom right). Representative images from 2 independent experiments.

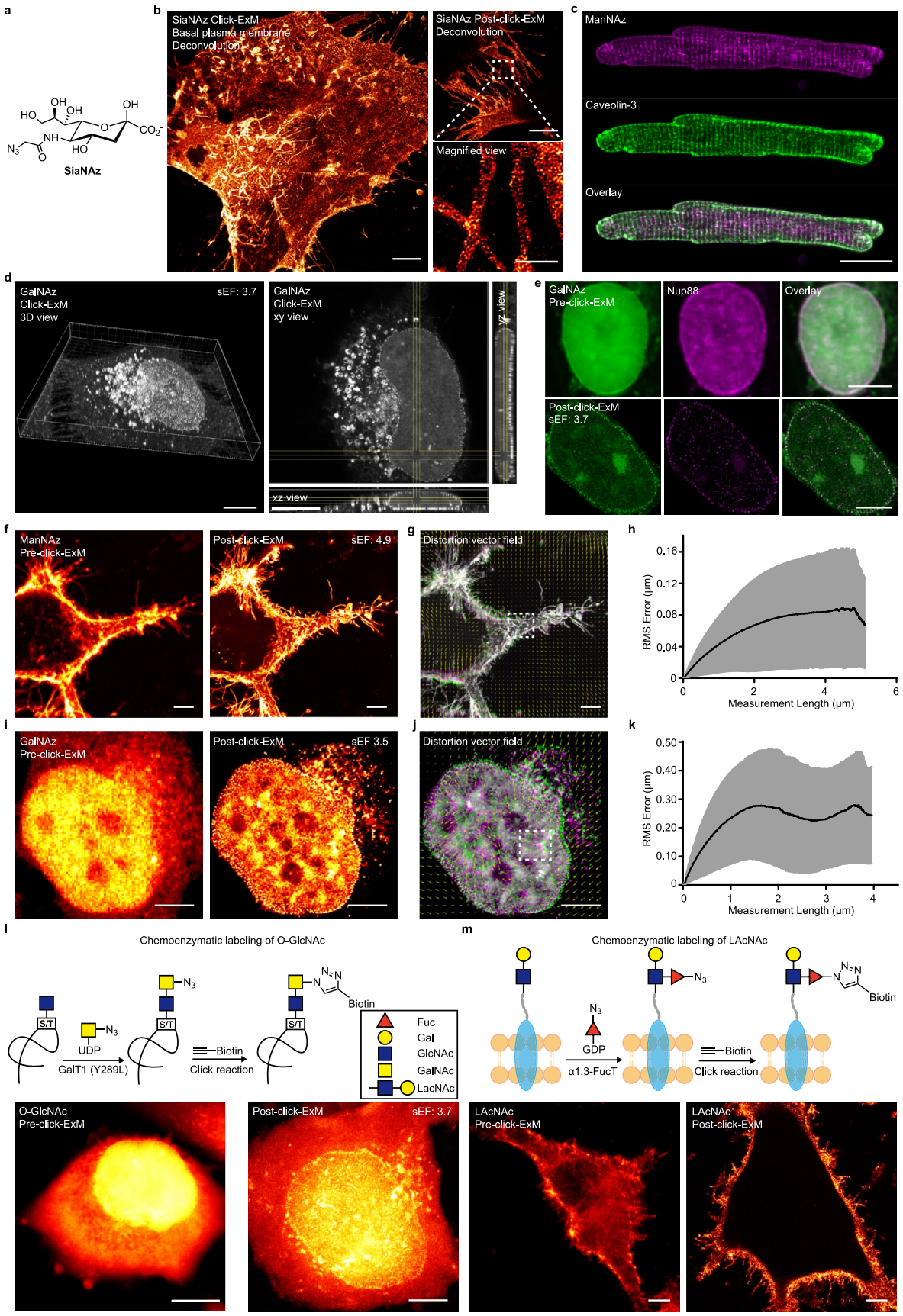

Extended Data Fig. 6 | See next page for caption.

Extended Data Fig. 6 | Pre- and post-click-ExM imaging of glycans (Related to Fig. 3). a, Chemical structure of SiaNAz. **b**, Click-ExM images of sialoglycans (AF555, red hot) in SiaNAz-treated HeLa cells after deconvolution. **c**, Confocal fluorescence images of rat cardiomyocytes, in which sialoglycans were metabolically labeled with ManNAz (AF555, magenta) and the T-tubule network was immunostained by using the T-tubule marker caveolin-3 (AF488, green). **d**, Click-ExM images of GalNAz-labeled HeLa cells (AF555, gray) shown in 3D (left) and xy, xz, yz views (right). **e**, Pre- and post-click-ExM images showing the colocalization between GalNAz-labeled glycans (AF488, green) and immunostained Nup88 (AF546, magenta) in CHO cells. **f**-**h**, Nanoscale isotropy of click-ExM for imaging of ManNAz-labeled sialoglycans. Pre- and post-click-ExM images (**f**, AF488, red hot) were aligned using rigid registration. Post-click-ExM images before and after non-rigid registration were overlaid and shown in green and magenta, respectively (**g**). The yellow arrows in **g** indicate the distortion vector field. From the boxed region in **g**, the RMS error was quantified as a function of measured distance (**h**), in which the black line indicates mean value and the grey area indicates ± s.d. **i**-**k**, Nanoscale isotropy of click-ExM for imaging of GalNAz-labeled glycans. Pre- and post-click-ExM images (**i**, AF555, red hot) were aligned using rigid registration. Post-click-ExM images before and after non-rigid registration were overlaid and shown in green and magenta, respectively (**j**). The yellow arrows in **j** indicate the distortion vector field. From the boxed region in **j**, the RMS error was quantified as a function of measured distance (**k**), in which the black line indicates mean value and the grey area indicates ± s.d. **l**, Pre- and post-click-ExM images of O-GlcNAc distribution chemoenzymatically labeled by Y289L GalT1 in CHO cells (AF555, red hot). **m**, Pre- and post-click-ExM images of LacNAc-containing glycans (AF488, red hot), which were chemoenzymatically labeled by α1,3-FucT in HeLa cells. Signal was amplified by iterative biotin trimer-streptavidin staining. Scale bars: 20 μm (**c**), 5 μm (**b**, **d**-**g**, **i**, **j**, **l**, **m**) and 1 μm (inset of **b**). All distances and scale bars correspond to the pre-expansion dimensions based on gEF (**b**, **m**) or sEF (**d**-**l**). AcX was used for anchoring. Analysis of isotropy from 2 (**f**-**k**) independent experiments. Representative images from ≥3 (**d**) or 2 (**b**, **c**, **e**, **l**, **m**) independent experiments.

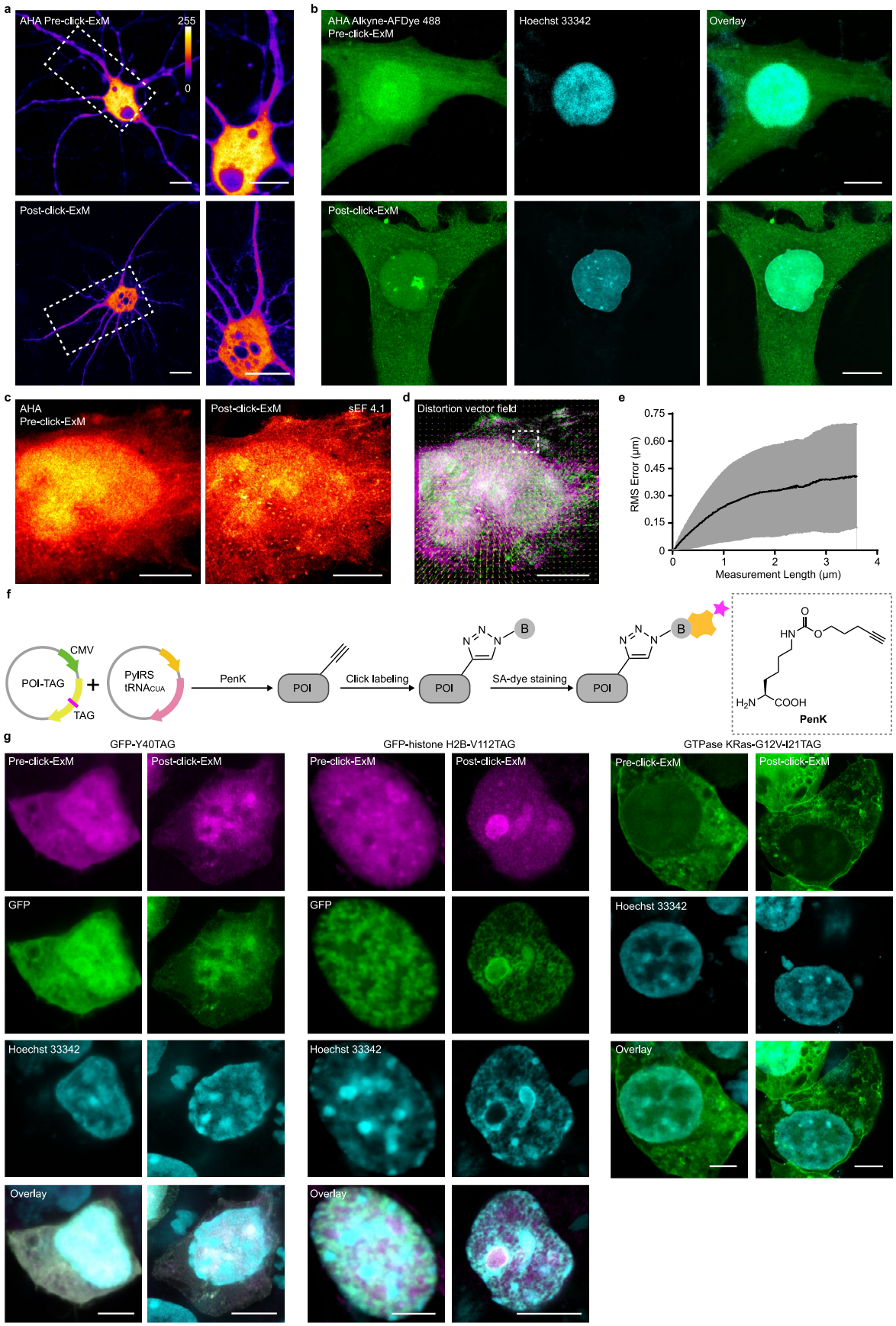

Extended Data Fig. 7 | See next page for caption.

Extended Data Fig. 7 | Pre- and post-click-ExM imaging of proteins (Related to Fig. 4a,b). a, Pre- and post-click-ExM images of nascent proteins in AHA-treated rat cortical neurons (Fire look-up table, AF488). **b**, Pre- and post-click-ExM images of HeLa cells treated with AHA, followed by direct click-labeling with alkyne-AFDye 488 (green). The nuclei were stained with Hoechst 33342 (cyan). **c**-**e**, Nanoscale isotropy of click-ExM for imaging of AHA-labeled proteins in U2OS cells. Pre- and post-click-ExM images (**c**, AF555, red hot) were aligned using rigid registration. Post-click-ExM images before and after non-rigid registration were overlaid and shown in green and magenta, respectively (**d**). The yellow arrows in **d** indicate the distortion vector field. From the boxed region in **d**, the RMS error was quantified as a function of measured distance (**e**), in which the black line indicates mean value and the grey area indicates ± s.d. **f**, Schematic of click-ExM on specific proteins labeled using the genetic code expansion strategy. The cells were co-transfected with the plasmid encoding a protein of interest bearing the amber codon (POI-TAG) and the plasmid encoding PenK-MbPylRS-tRNA$_{pyl\ CUA}$ in the presence of the Pyl analogue (PenK), followed by the click-ExM procedure. **g**, Pre- and post-click-ExM images of GFP (AF555, magenta, HEK293T), GFP-histone H2B (AF555, magenta, COS-7) and GTPase KRas (AF488, green, HEK293T). For GFP and GFP-histone H2B, GFP channels were also shown (green). The nuclei were stained with Hoechst 33342 (cyan). Scale bars: 10 μm (**a**-**d**) and 5 μm (**g**). All distances and scale bars correspond to the pre-expansion dimensions based on gEF (**a**, **b**, **g**) or sEF (**c**-**e**). AcX was used for anchoring. Analysis of isotropy from 1 (**c**-**e**) independent experiment. Representative images from ≥3 (**a**, pre-click-ExM of **g**), 2 (post-click-ExM images of GFP in **g**) or 1 (**b**, post-click-ExM images of histone H2B and GTPase KRas in **g**) independent experiments.

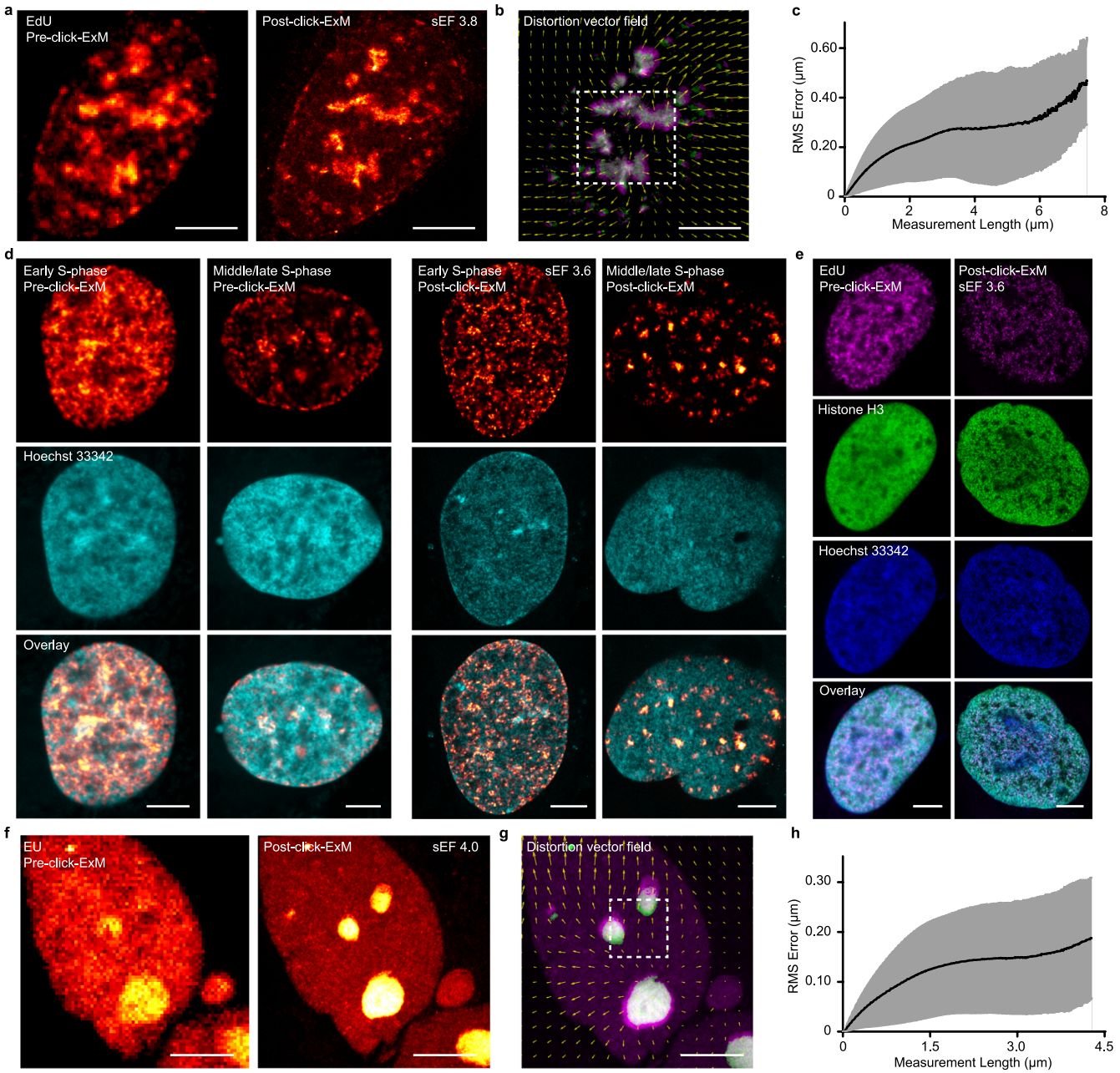

Extended Data Fig. 8 | Pre- and post-click-ExM imaging of EdU-labeled nascent DNA and EU-labeled nascent RNA (Related to Fig. 4c,d). a-c, Nanoscale isotropy of click-ExM for imaging of EdU-labeled DNA. Pre- and post-click-ExM images (**a**, AF488, red hot) were aligned using rigid registration. Post-click-ExM images before and after non-rigid registration were overlaid and shown in green and magenta, respectively (**b**). The yellow arrows in **b** indicate the distortion vector field. From the boxed region in **b**, the RMS error was quantified as a function of measured distance (**c**), in which the black line indicates mean value and the grey area indicates ± s.d. The same images were shown in Fig. 4c. **d**, In U2OS cells, pre- and post-click-ExM images of EdU-labeled nascent DNA (AF555, red hot) in early and middle/late S-phase, from which chromatins with different sizes and shapes were observed. The nuclei were stained with Hoechst 33342 (cyan). **e**, Click-ExM images showing colocalization of EdU-labeled nascent DNA (AF555, magenta) with immunostained histone H3 (AF488, green). The nuclei were stained with Hoechst 33342 (blue). **f-h**, Nanoscale isotropy of click-ExM for imaging of EU-labeled RNA. Pre- and post-click-ExM images (**f**, AF555, red hot) were aligned using rigid registration. Post-click-ExM images before and after non-rigid registration were overlaid and shown in green and magenta, respectively (**g**). The yellow arrows in **g** indicate the distortion vector field. From the boxed region in **g**, the RMS error was quantified as a function of measured distance (**h**), in which the black line indicates mean value and the grey area indicates ± s.d. The same regions were shown in Fig. 4d. Scale bars: 5 μm. All distances and scale bars correspond to the pre-expansion dimensions based on sEF. AcX was used for anchoring. Analysis of isotropy from 2 (**a-c**, **f-h**) independent experiments. Representative images from ≥3 (**d**), 2 (pre-click-ExM images of **e**) or 1 (post-click-ExM images of **e**) independent experiments.

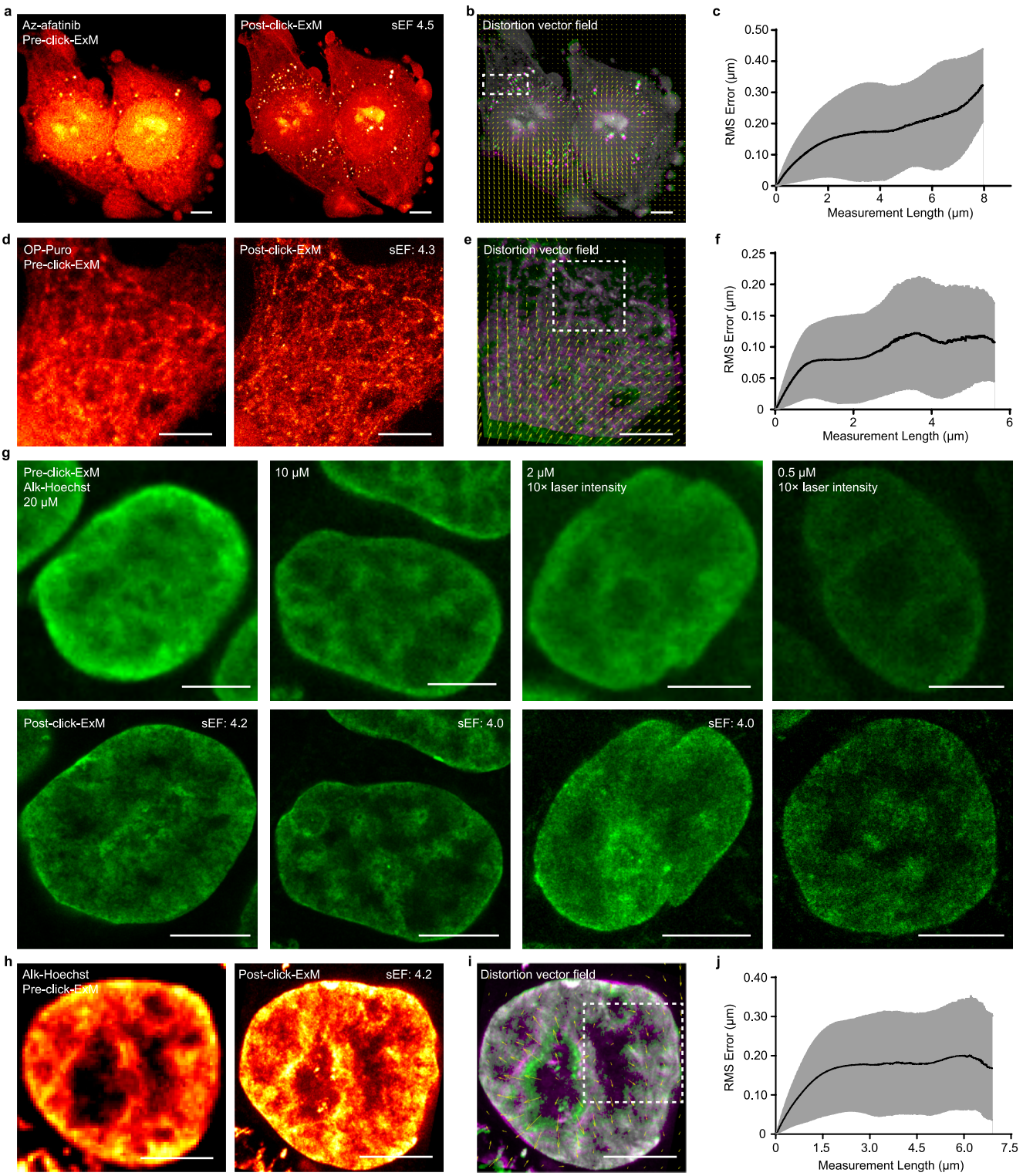

Extended Data Fig. 9 | See next page for caption.

Extended Data Fig. 9 | Pre- and post-click-ExM imaging of small molecules (Related to Fig. 4e-g). a-c, Nanoscale isotropy of click-ExM for imaging of HeLa cells treated with Az-afatinib. Pre- and post-click-ExM images (**a**, AF555, red hot) were aligned using rigid registration. Post-click-ExM images before and after non-rigid registration were overlaid and shown in green and magenta, respectively (**b**). The yellow arrows in **b** indicate the distortion vector field. From the boxed region in **b**, the RMS error was quantified as a function of measured distance (**c**), in which the black line indicates mean value and the grey area indicates ± s.d. The same images were shown in Fig. 4e. (**d-f**) Nanoscale isotropy of click-ExM for imaging of HeLa cells treated with OP-Puro. Pre- and post-click-ExM images (**d**, AF488, red hot) were aligned using rigid registration. Post-click-ExM images before and after non-rigid registration were overlaid and shown in green and magenta, respectively (**e**). The yellow arrows in **e** indicate the distortion vector field. From the boxed region in **e**, the RMS error was quantified as a function of measured distance (**f**), in which the black line indicates mean value and the grey area indicates ± s.d. The same regions were shown in Fig. 4f. **g**, HeLa cells were labeled with Alk-Hoechst at varied concentrations (0.5–20 μM, AF488, green). The same cells were imaged before and after expansion for comparison except the 0.5 μM group. The same images of the 10 μM group were shown in Fig. 4g. Representative images from 2 independent experiments except 20 μM group (1 independent experiment). **h-j**, Nanoscale isotropy of click-ExM for imaging of HeLa cells labeled with Alk-Hoechst. Pre- and post-click-ExM images (**h**, AF488, red hot) were aligned using rigid registration. Post-click-ExM images before and after non-rigid registration were overlaid and shown in green and magenta, respectively (**i**). The yellow arrows in **i** indicate the distortion vector field. From the boxed region in **i**, the RMS error was quantified as a function of measured distance (**j**), in which the black line indicates mean value and the grey area indicates ± s.d. Scale bars: 5 μm. AcX was used for anchoring. All distances and scale bars correspond to the pre-expansion dimensions based on sEF and gEF (0.5 μM group in **g**). Analysis of isotropy from 2 (**d-f**, **h-j**) or 1 (**a-c**) independent experiments.

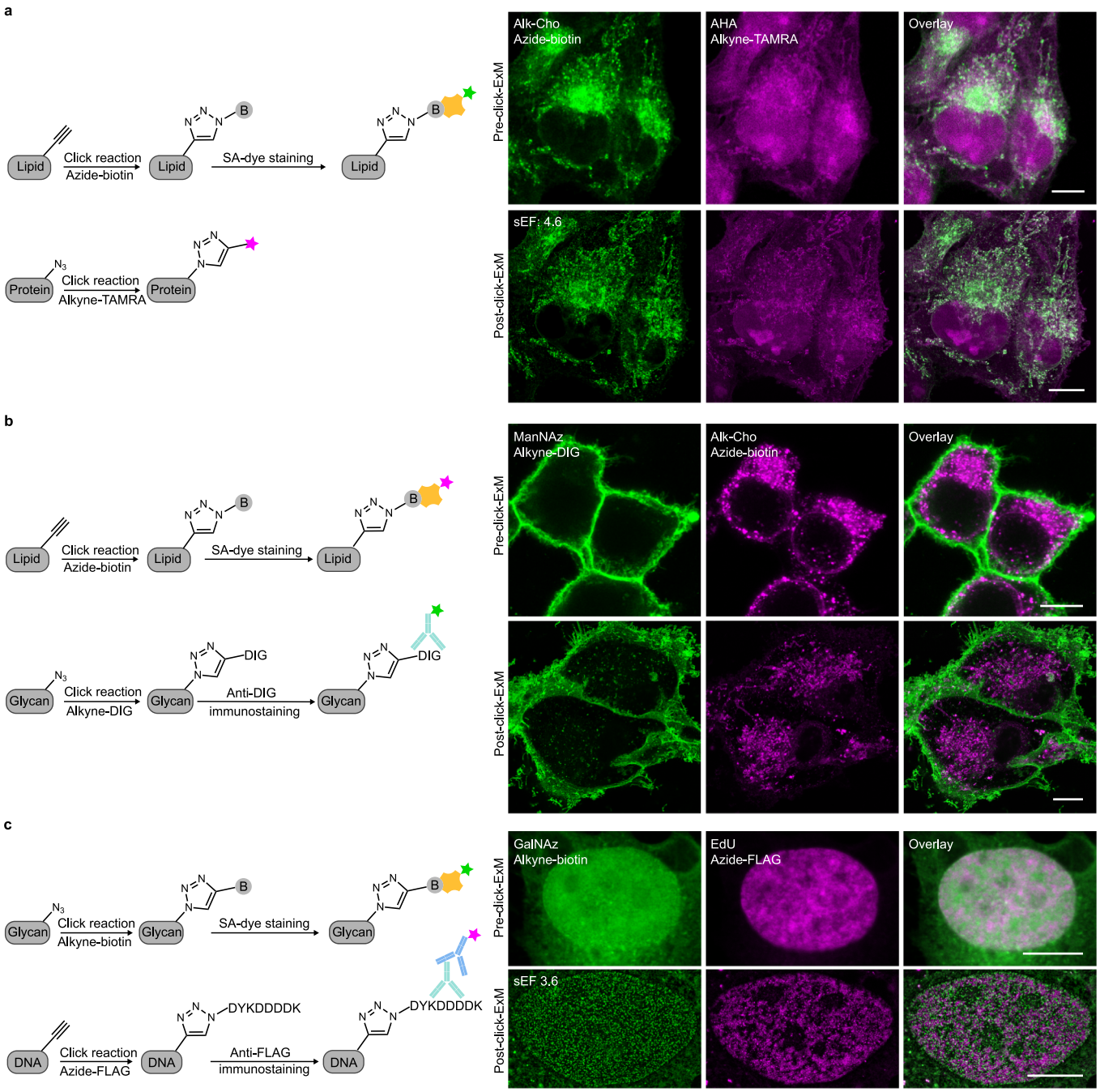

Extended Data Fig. 10 | Multicolor click-ExM imaging of different biomolecules. a, Two-color click-ExM imaging of lipids and proteins. COS-7 cells were simultaneously treated with Alk-Cho and AHA. The alkyne-incorporated lipids were reacted with azide-biotin and stained with SA-AF488 (green). The azide-incorporated proteins were reacted with alkyne-TAMRA (magenta). **b**, Two-color click-ExM imaging of lipids and glycans. COS-7 cells were simultaneously treated with ManNAz and Alk-Cho. The alkyne-incorporated lipids were reacted with azide-biotin and stained with SA-AF555 (magenta). The azide-incorporated glycans were reacted with alkyne-DIG and immunostained with DyLight 488-conjugated anti-DIG antibody (green). **c**, Two-color click-ExM imaging of glycans and DNA. HeLa cells were simultaneously treated with GalNAz and EdU. The azide-incorporated glycans was reacted with alkyne-biotin and stained with SA-AF488 (green). The alkyne-incorporated nascent DNA was reacted with azide-FLAG and immunostained with anti-FLAG antibody (AF555, magenta). AcX was used for anchoring. Scale bars: 10 μm. All scale bars correspond to the pre-expansion dimensions based on gEF (**b**) or sEF (**a**, **c**). Representative images from ≥3 (pre-click-ExM images of **a**, **c**), 2 (pre-click-ExM images of **b** and post-click-ExM images of **a**) or 1 (post-click-ExM images of **b**, **c**) independent experiments.

nature research

Corresponding author(s): Xing Chen

Last updated by author(s): Oct 18, 2020

Reporting Summary

Nature Research wishes to improve the reproducibility of the work that we publish. This form provides structure for consistency and transparency in reporting. For further information on Nature Research policies, see our Editorial Policies and the Editorial Policy Checklist.

Statistics

For all statistical analyses, confirm that the following items are present in the figure legend, table legend, main text, or Methods section.

n/a	Confirmed	
☐	☒	The exact sample size (*n*) for each experimental group/condition, given as a discrete number and unit of measurement
☐	☒	A statement on whether measurements were taken from distinct samples or whether the same sample was measured repeatedly
☐	☒	The statistical test(s) used AND whether they are one- or two-sided *Only common tests should be described solely by name; describe more complex techniques in the Methods section.*
☒	☐	A description of all covariates tested
☒	☐	A description of any assumptions or corrections, such as tests of normality and adjustment for multiple comparisons
☐	☒	A full description of the statistical parameters including central tendency (e.g. means) or other basic estimates (e.g. regression coefficient) AND variation (e.g. standard deviation) or associated estimates of uncertainty (e.g. confidence intervals)
☐	☒	For null hypothesis testing, the test statistic (e.g. *F*, *t*, *r*) with confidence intervals, effect sizes, degrees of freedom and *P* value noted *Give P values as exact values whenever suitable.*
☒	☐	For Bayesian analysis, information on the choice of priors and Markov chain Monte Carlo settings
☒	☐	For hierarchical and complex designs, identification of the appropriate level for tests and full reporting of outcomes
☒	☐	Estimates of effect sizes (e.g. Cohen's *d*, Pearson's *r*), indicating how they were calculated

Our web collection on statistics for biologists contains articles on many of the points above.

Software and code

Policy information about availability of computer code

Data collection	Imaging data collection was performed on commercial microscopes detailed in the manuscript and collected by ZEN 2011 (v 8.0.0.273), ZEN 3.0 SR Black (16.0.3.306), ZEN 3.0 Blue (3.0.79.00005), LAS X 2.0.1.14392, LAS X 3.5.2.18963, LAS X 3.5.5.19976, and NIS-Elements BR 4.60.00 64-bit. Image of Coomassie Brilliant Blue-stained gel was collected on a ChemiDoc XRS+ (Bio-Rad). 1H NMR and 13C NMR spectra were recorded on a Bruker-400 MHz NMR (ARX400) and Bruker-500 MHz NMR (AVANCE III) instrument. High-resolution mass spectra (HRMS) were recorded on a Fourier Transform Ion Cyclotron Resonance Mass Spectrometer (APEX IV). MALDI-TOF mass spectra were recodred on a MALDI-TOF/TOF Mass Spectrometer (AB Sciex 5800).
Data analysis	Fiji/ImageJ v1.52p, Imaris v9.0.2, Matlab R2018a and Huygens Professional v17.10 were used for image analysis. PyMOL Molecular Graphics System v1.8.2.2 was used for crystal structure visualization. ChemDraw Professional v19.1.0.5 was used to draw chemical structures. GraphPad Prism 7.0 and Origin Pro 2019b were used for statistics. Adobe illustrator 2020 v24.3 was used for graph assembling.

For manuscripts utilizing custom algorithms or software that are central to the research but not yet described in published literature, software must be made available to editors and reviewers. We strongly encourage code deposition in a community repository (e.g. GitHub). See the Nature Research guidelines for submitting code & software for further information.

Data

Policy information about availability of data

All manuscripts must include a data availability statement. This statement should provide the following information, where applicable:

- Accession codes, unique identifiers, or web links for publicly available datasets
- A list of figures that have associated raw data
- A description of any restrictions on data availability

Source data for Figs. 2c, e, g, j, 3d, g, h, Extended data Figs. 1c, e, f, i, j, 3f, 5c, 6h, k, 7e, 8c, h, and 9c, f, j are available online as Source Data File. The Matlab codes and examples for registration and distortion analysis are available from GitHub (https://github.com/Yujie-S/Click-ExM_data_process_and_example). All other data in this study are available from the corresponding author upon reasonable request.

Field-specific reporting

Please select the one below that is the best fit for your research. If you are not sure, read the appropriate sections before making your selection.

☒ Life sciences ☐ Behavioural & social sciences ☐ Ecological, evolutionary & environmental sciences

For a reference copy of the document with all sections, see nature.com/documents/nr-reporting-summary-flat.pdf

Life sciences study design

All studies must disclose on these points even when the disclosure is negative.

Sample size	The sample size was not pre-determined. The sample size was chosen based on our prior experience on similar experiments and literature reports (e.g., Gambarotto, Davide, et al. Nature Methods, 2019,16, 71-74), which could adequately demonstrate the performance of our method.
Data exclusions	The exclusion criteria were pre-established: in Supplementary Note Figure 1b, images cannot be matched before and after click-ExM process due to out-of-focus blur were not included in the analysis.
Replication	Replication was successful in all cases. The exact number of independent experiments are provided in the figure legends.
Randomization	Rats and mice were randomly selected before further treatment. Other experiments were not randomized, because randomization was considered to be not necessary as the purpose of the study was to demonstrate a new method and not to report biological findings.
Blinding	Blinding was not performed during the method development. Our experimental workflow did not allow blinding, because imaging conditions had to be adjusted according to samples.

Reporting for specific materials, systems and methods

We require information from authors about some types of materials, experimental systems and methods used in many studies. Here, indicate whether each material, system or method listed is relevant to your study. If you are not sure if a list item applies to your research, read the appropriate section before selecting a response.

Materials & experimental systems

n/a	Involved in the study
☐	☒ Antibodies
☐	☒ Eukaryotic cell lines
☒	☐ Palaeontology and archaeology
☐	☒ Animals and other organisms
☒	☐ Human research participants
☒	☐ Clinical data
☒	☐ Dual use research of concern

Methods

n/a	Involved in the study
☒	☐ ChIP-seq
☒	☐ Flow cytometry
☒	☐ MRI-based neuroimaging

Antibodies

Antibodies used	Commerical primary antibodies: anti-alpha-tubulin (Abcam, ab52866, 1:250), anti-Tom20 (Abcam, ab186734, 1:250),anti-Nup88 (Santa Cruz, sc-365868, 1:100), anti-Histone H3 (Abcam, ab176842, 1:2,000), anti-FLAG tag (Abcam, ab205606, 1:100), anti-caveolin-3 (Santa Cruz, sc-5310, 1:50) Commerical secondary antibodies: goat anti-mouse secondary antibody, Alexa Fluor 488 (Thermo, A-11001, 1:500), goat anti-mouse secondary antibody, Alexa Fluor 546 (Thermo, A-11003, 1:500), goat anti-rabbit secondary antibody, Alexa Fluor 488 (Thermo, A-11034, 1:200), goat anti-rabbit secondary antibody, Alexa Fluor 555 (Thermo, A-21429, 1:500), goat anti-rabbit secondary antibody, Alexa Fluor 647 (Thermo,

A-21245, 1:1,000), goat anti-DIG antibody, DyLight 488 (Vectorlabs, DI-7488, 1:100) and biotinylated goat anti-rabbit secondary antibody (Proteintech, SA00004-2, 1:200).

Validation

All antibodies are validated by vendors indicated above. Many references are listed on respective manufactures' websites. Below we list one reference for each antibody.

anti-alpha-tublin DOI: 10.1038/nsmb.2638
anti-Tom20 DOI: 10.1038/s41592-018-0238-1
anti-Nup88 DOI: 10.1172/JCI82277
anti-Histone H3 DOI: 10.1038/s41467-017-00694-2
anti-FLAG tag DOI: 10.1126/sciadv.aay8627
anti-caveolin-3 DOI: 10.1161/CIRCRESAHA.117.310996
goat anti-mouse secondary antibody, Alexa Fluor 488 DOI: 10.1038/nmeth.2972
goat anti-mouse secondary antibody, Alexa Fluor 546 DOI: 10.1016/j.cell.2020.01.011.
goat anti-rabbit secondary antibody, Alexa Fluor 488 DOI: 10.1038/s41377-020-0295-y
goat anti-rabbit secondary antibody, Alexa Fluor 555 DOI: 10.1073/pnas.1705623114
goat anti-rabbit secondary antibody, Alexa Fluor 647 DOI: 10.1038/nmeth.3964
goat anti-DIG antibody, DyLight 488 DOI: 10.1093/nar/gkz376
biotinylated goat anti-rabbit secondary antibody DOI: 10.1093/hmg/ddv439

Eukaryotic cell lines

Policy information about cell lines

Cell line source(s)

HeLa (ATCC, CCL-2), HEK293T (ATCC, CRL-11268) and CHO (ATCC, CCL-61) were obtained from American Type Culture Collection.
U2OS (3111C0001CCC000028, National Infrastructure of Cell Line Resource, Beijing, China)
COS-7 (Cell Bank, Chinese Academy of Science, Shanghai, China)

Authentication

The cell lines were frequently checked by their morphological features and no further authentication was performed.

Mycoplasma contamination

All cell lines were tested negative for mycoplasma contamination.

Commonly misidentified lines
(See ICLAC register)

No commonly misidentified cell lines were used.

Animals and other organisms

Policy information about studies involving animals; ARRIVE guidelines recommended for reporting animal research

Laboratory animals

Male and female Sprague-Dawley rats (postnatal day 0, P0) for preparing hippocampal and cortical neurons, male Sprague-Dawley rats (~2 months) for preparing cardiomyocytes, male C57BL/6N mice (P21-27) for preparing acute brain slices were purchased from Vital River Laboratory Animal Center (Beijing, China) and kept under specific-pathogen-free (SPF) condition. Animals were housed in the temperature-controlled animal room (~24 degrees centigrade, humidity 50-60%) with a 12-h light/12-h dark cycle.

Wild animals

The study did not involve wild animals.

Field-collected samples

The study did not involve samples collected from field.

Ethics oversight

All animal experiments were performed in accordance with guidelines approved by the Institutional Animal Care and Use Committee of Peking University accredited by AAALAC International.

Note that full information on the approval of the study protocol must also be provided in the manuscript.